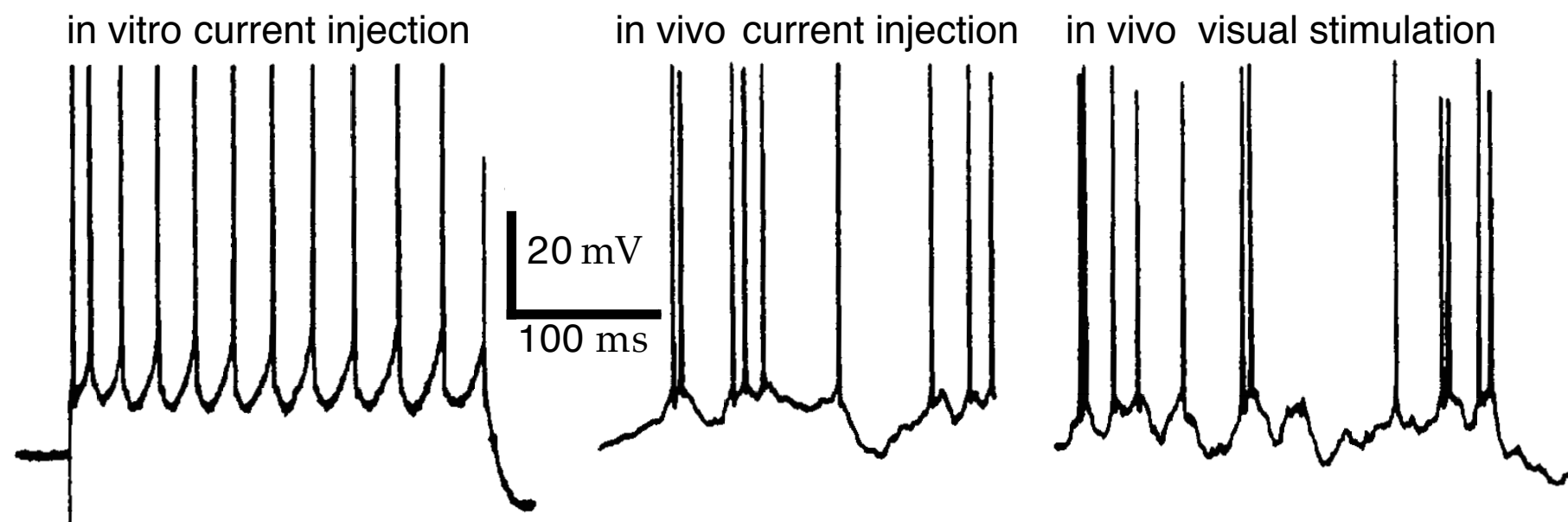


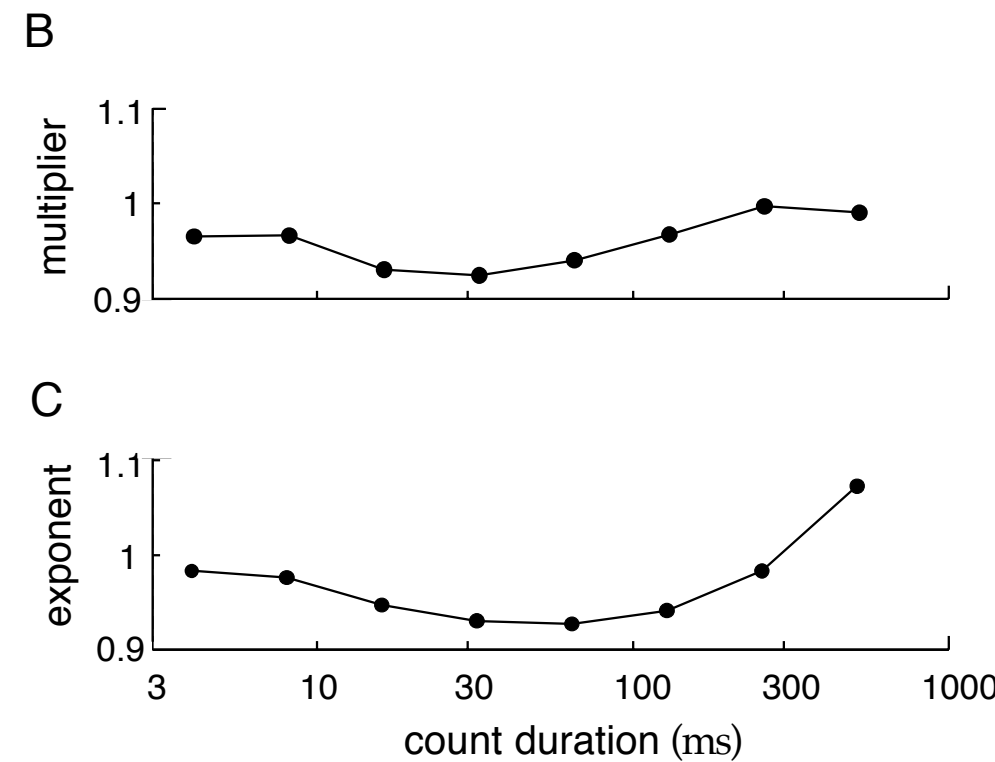
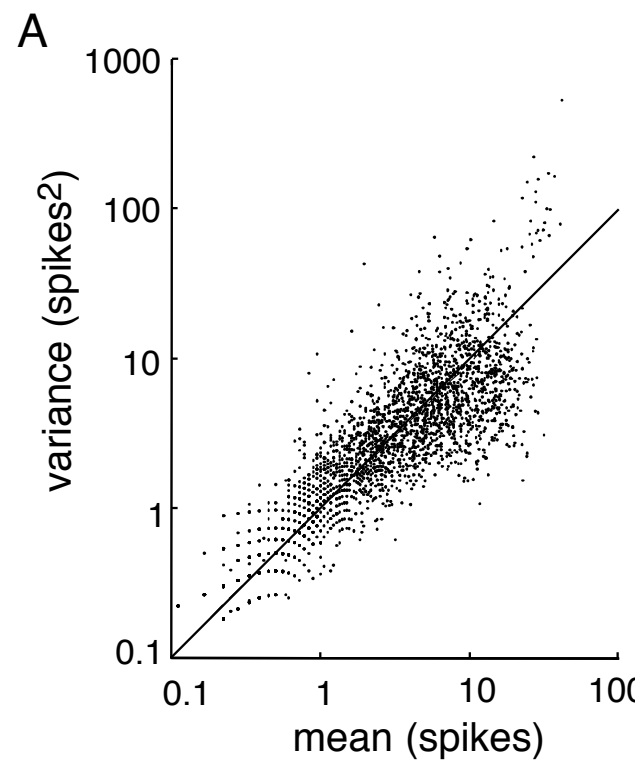
Encoding

Statistics of Spike trains



$$\rho(t) = \sum_i \delta(t - t_i)$$

Testing the Poisson Model



Testing the Poisson Model

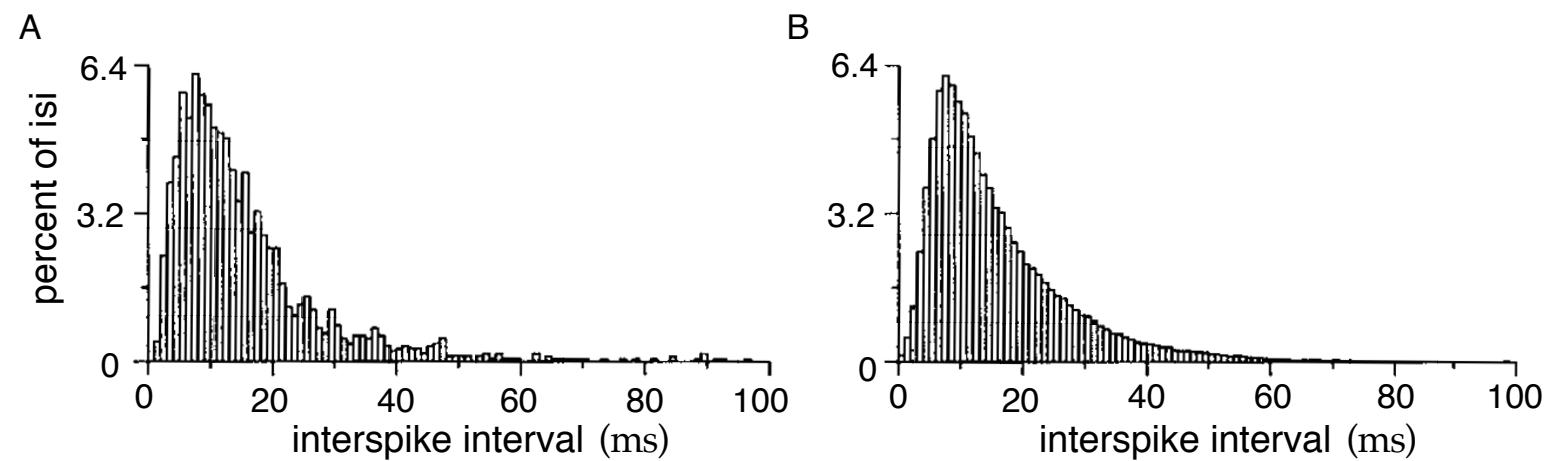
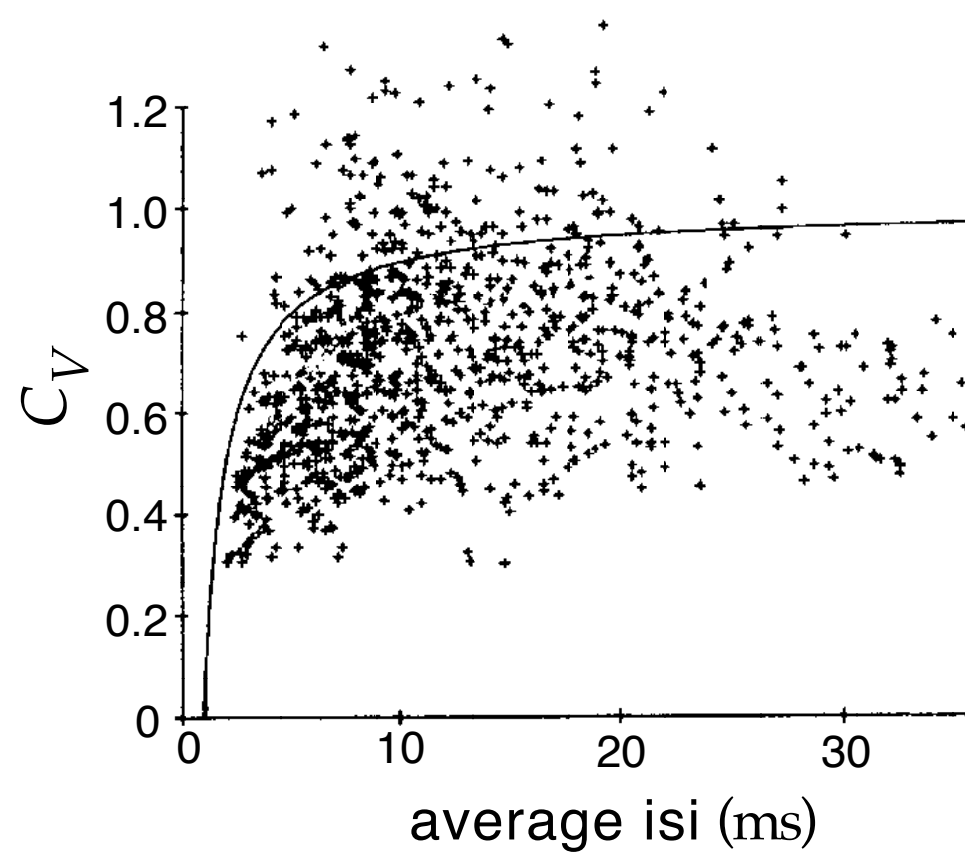
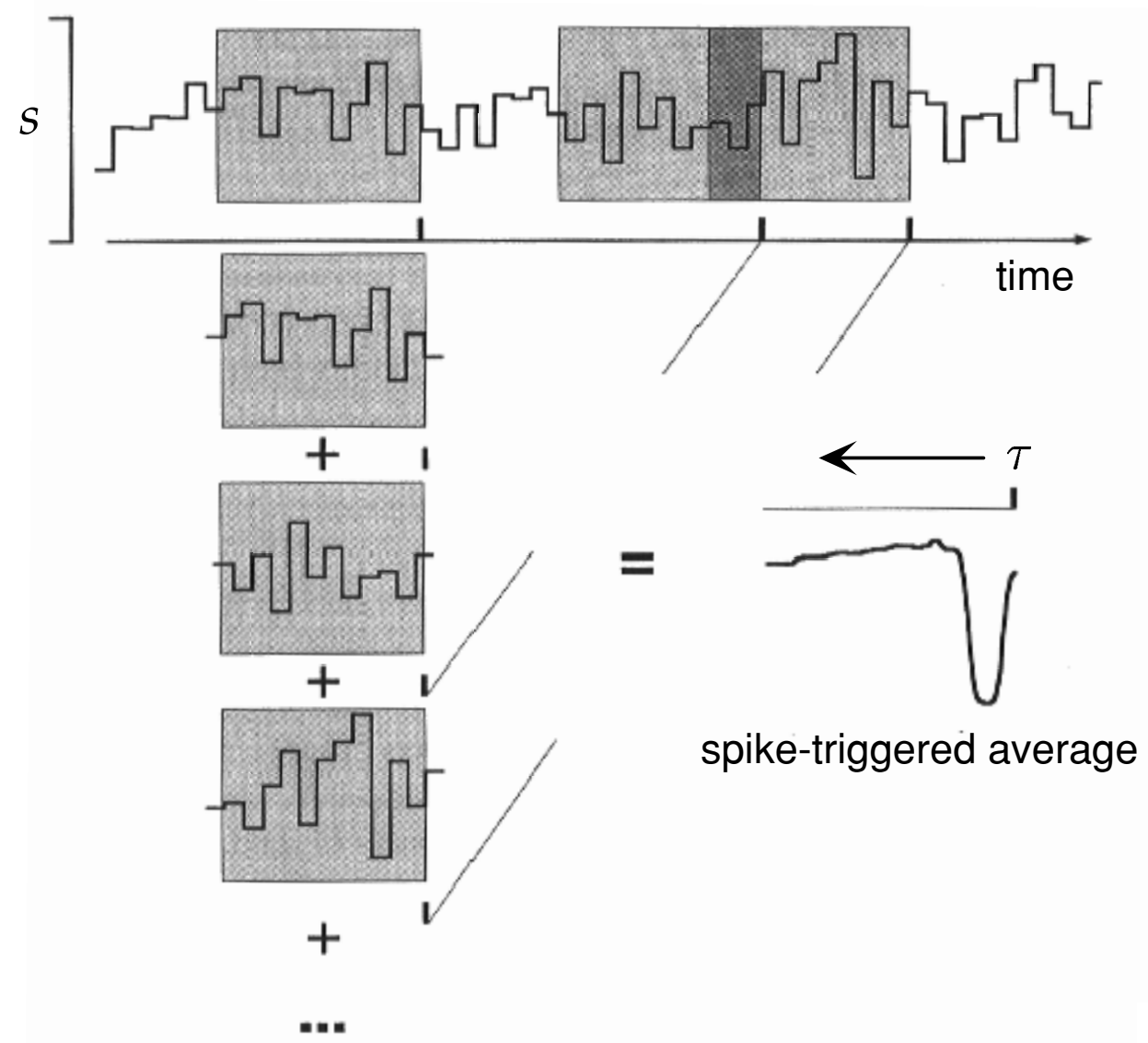
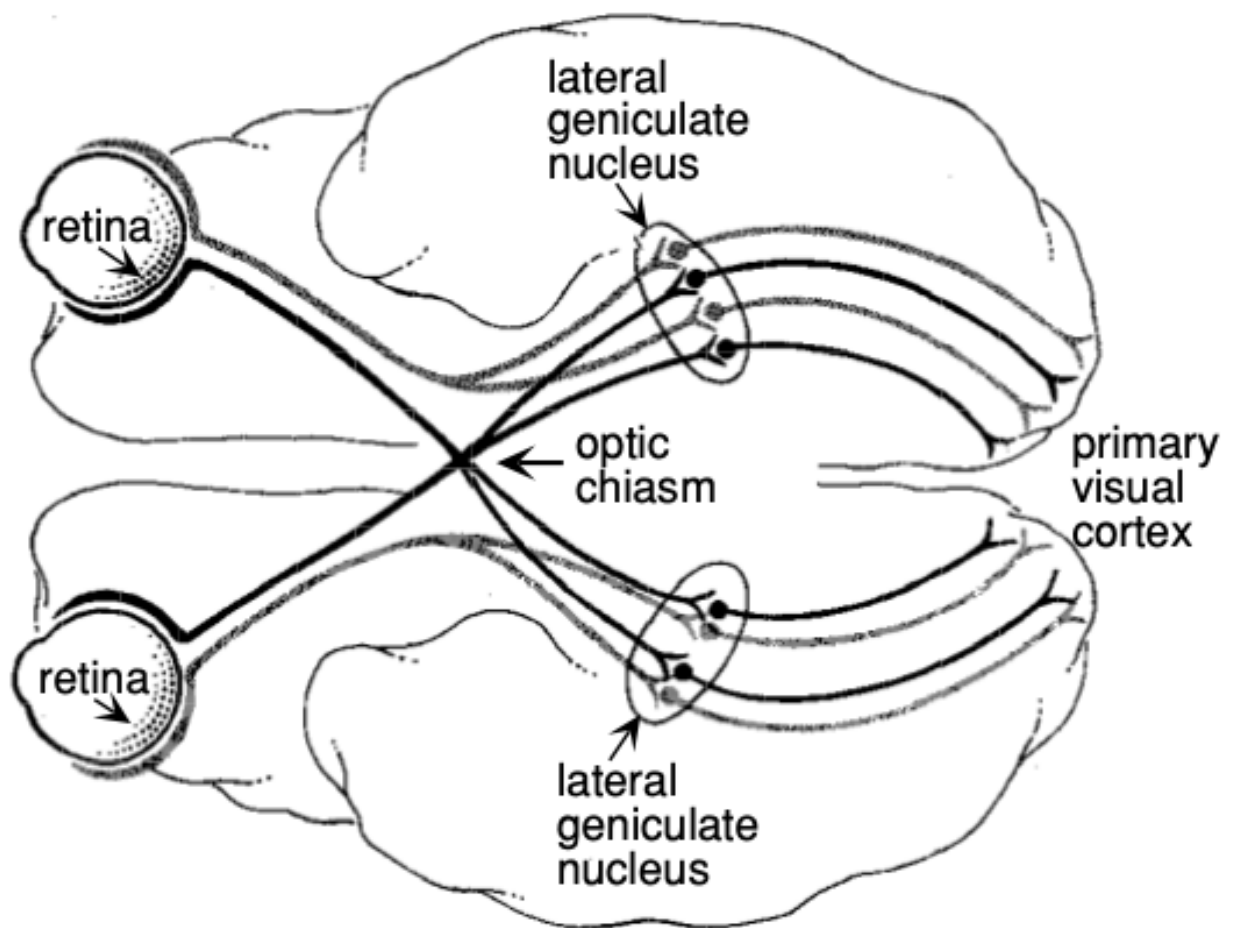


Figure 1.15: (A) Interspike interval distribution from an MT neuron responding to a moving random dot image. The probability of interspike intervals falling into the different bins, expressed as a percentage, is plotted against interspike interval. B) Interspike interval histogram generated from a Poisson model with a stochastic refractory period. (Adapted from Bair et al., 1994.)

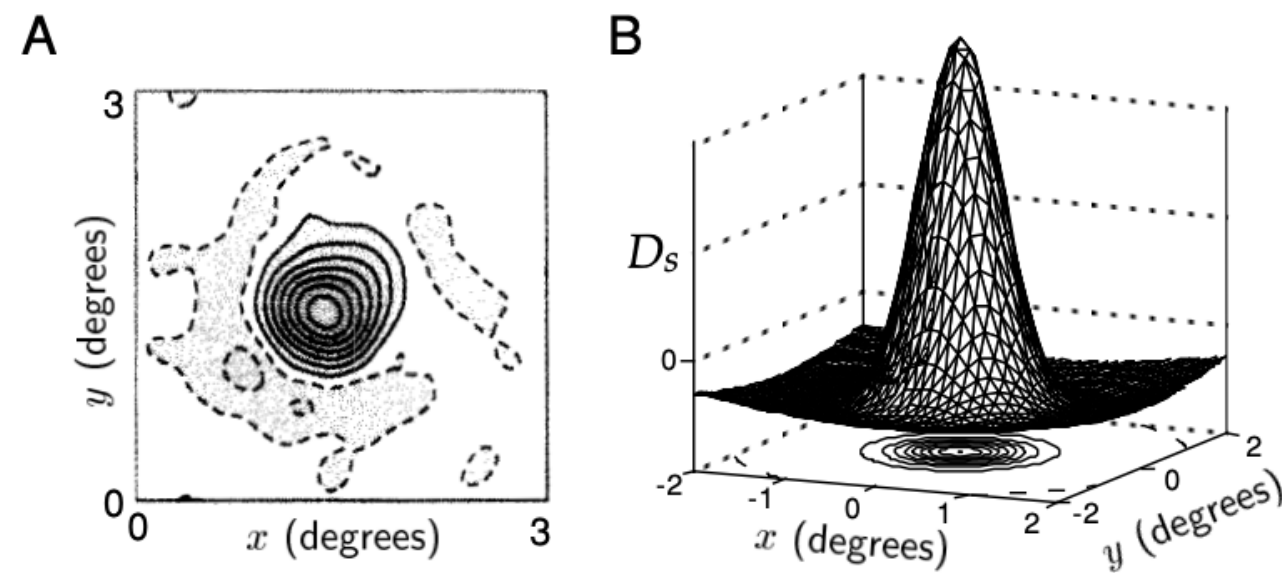
Testing the Poisson Model







Receptive field of retinal ganglion cells



Differences between Gaussians

$$D_s(x, y) = \pm \left(\frac{1}{2\pi\sigma_{\text{cen}}^2} \exp\left(-\frac{x^2 + y^2}{2\sigma_{\text{cen}}^2}\right) - \frac{B}{2\pi\sigma_{\text{sur}}^2} \exp\left(-\frac{x^2 + y^2}{2\sigma_{\text{sur}}^2}\right) \right).$$

Receptive field of simple cells in the visual cortex

$$D_s(x, y) = \frac{1}{2\pi\sigma_x\sigma_y} \exp\left(-\frac{x^2}{2\sigma_x^2} - \frac{y^2}{2\sigma_y^2}\right) \cos(kx - \phi)$$

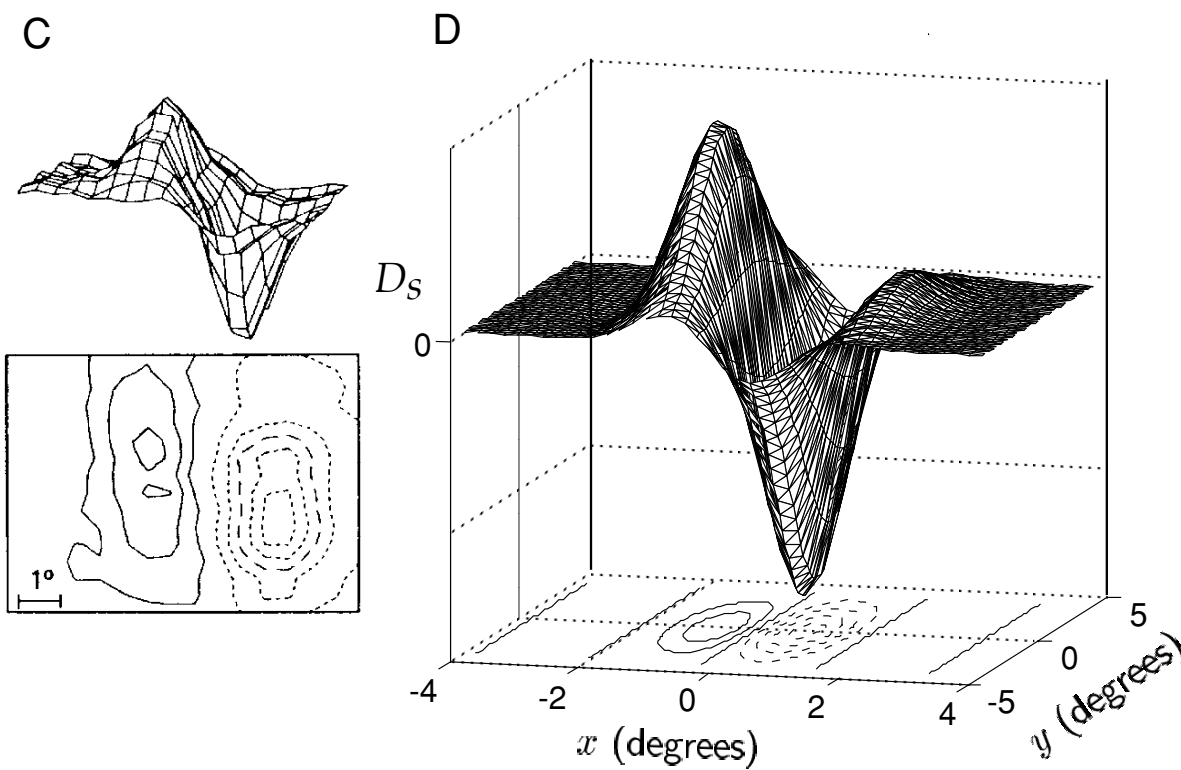


Figure 2.10 Spatial receptive field structure of simple cells. (A) and (C) Spatial structure of the receptive fields of two neurons in cat primary visual cortex determined by averaging stimuli between 50 ms and 100 ms prior to an action potential. The upper plots are three-dimensional representations, with the horizontal dimensions acting as the x - y plane and the vertical dimension indicating the magnitude and sign of $D_s(x, y)$. The lower contour plots represent the x - y plane. Regions with solid contour curves are ON areas where $D_s(x, y) > 0$, and regions with dashed contours are OFF areas where $D_s(x, y) < 0$. (B) and (D) Gabor functions (equation 2.27) with $\sigma_x = 1^\circ$, $\sigma_y = 2^\circ$, $1/k = 0.56^\circ$, and $\phi = 1 - \pi/2$ (B) or $\phi = 1 - \pi$ (D), chosen to match the receptive fields in A and C. (A and C adapted from Jones and Palmer, 1987a.)

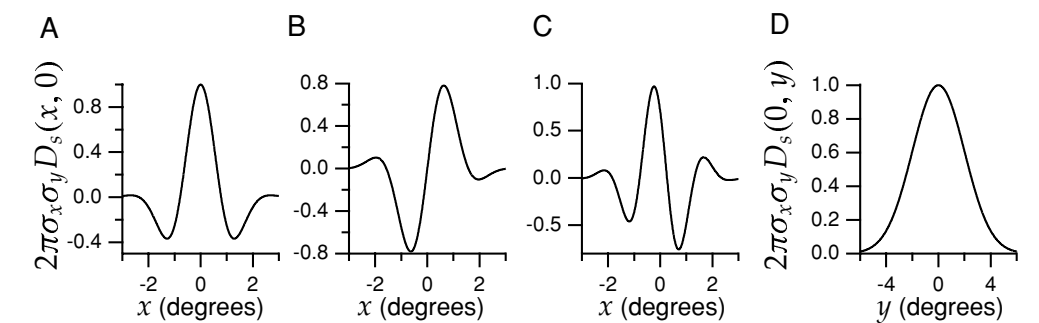
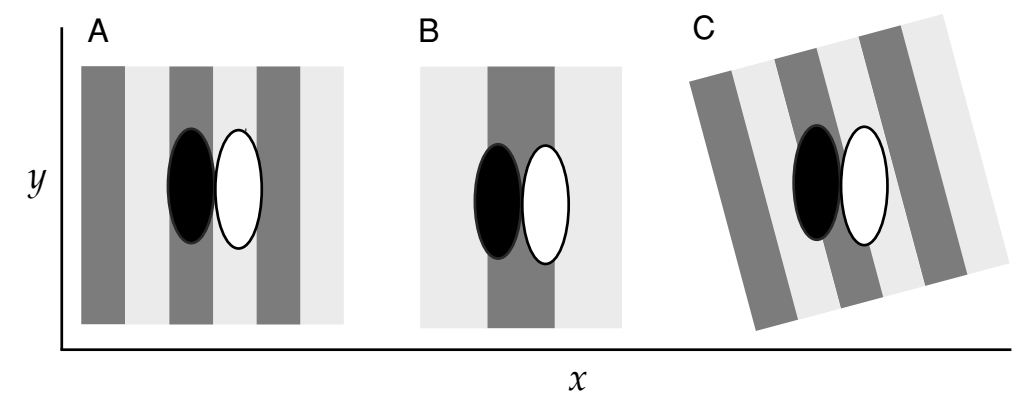


Figure 2.12 Gabor functions of the form given by equation 2.27. For convenience we plot the dimensionless function $2\pi\sigma_x\sigma_y D_s$. (A) A Gabor function with $\sigma_x = 1^\circ$, $1/k = 0.5^\circ$, and $\phi = 0$ plotted as a function of x for $y = 0$. This function is symmetric about $x = 0$. (B) A Gabor function with $\sigma_x = 1^\circ$, $1/k = 0.5^\circ$, and $\phi = \pi/2$ plotted as a function of x for $y = 0$. This function is antisymmetric about $x = 0$ and corresponds to using a sine instead of a cosine function in equation 2.27. (C) A Gabor function with $\sigma_x = 1^\circ$, $1/k = 0.33^\circ$, and $\phi = \pi/4$ plotted as a function of x for $y = 0$. This function has no particular symmetry properties with respect to $x = 0$. (D) The Gabor function of equation 2.27 with $\sigma_y = 2^\circ$ plotted as a function of y for $x = 0$. This function is simply a Gaussian.

Hubel-Wiesel model of orientation selectivity

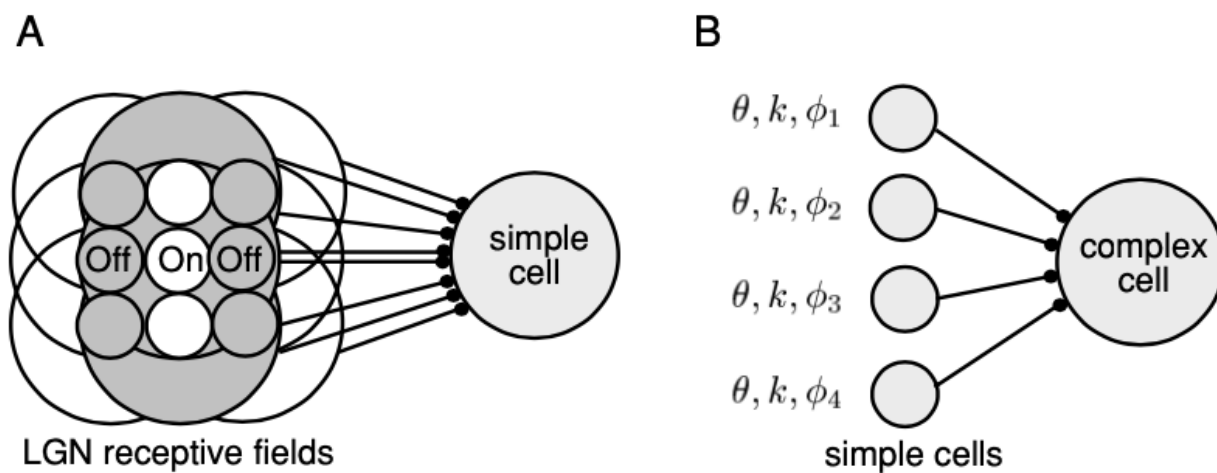


Figure 2.27 (A) The Hubel-Wiesel model of orientation selectivity. The spatial arrangement of the receptive fields of nine LGN neurons are shown, with a row of three ON-center fields flanked on either side by rows of three OFF-center fields. White areas denote ON fields and gray areas, OFF fields. In the model, the converging LGN inputs are summed by the simple cell. This arrangement produces a receptive field oriented in the vertical direction. (B) The Hubel-Wiesel model of a complex cell. Inputs from a number of simple cells with similar orientation and spatial frequency preferences (θ and k), but different spatial phase preferences (ϕ_1, ϕ_2, ϕ_3 , and ϕ_4), converge on a complex cell and are summed. This produces a complex cell output that is selective for orientation and spatial frequency, but not for spatial phase. The figure shows four simple cells converging on a complex cell, but additional simple cells can be included to give a more complete coverage of spatial phase.

Temporal receptive field

$$D_t(\tau) = \alpha \exp(-\alpha\tau) \left[\frac{(\alpha\tau)^5}{5!} - \frac{(\alpha\tau)^7}{7!} \right]$$

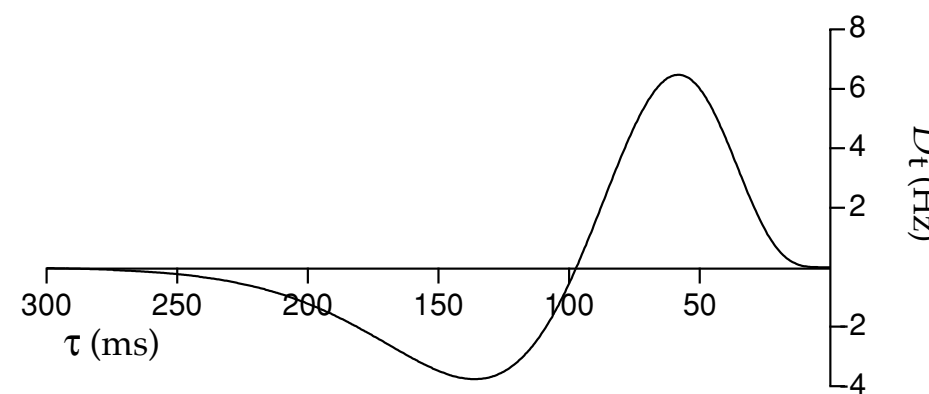
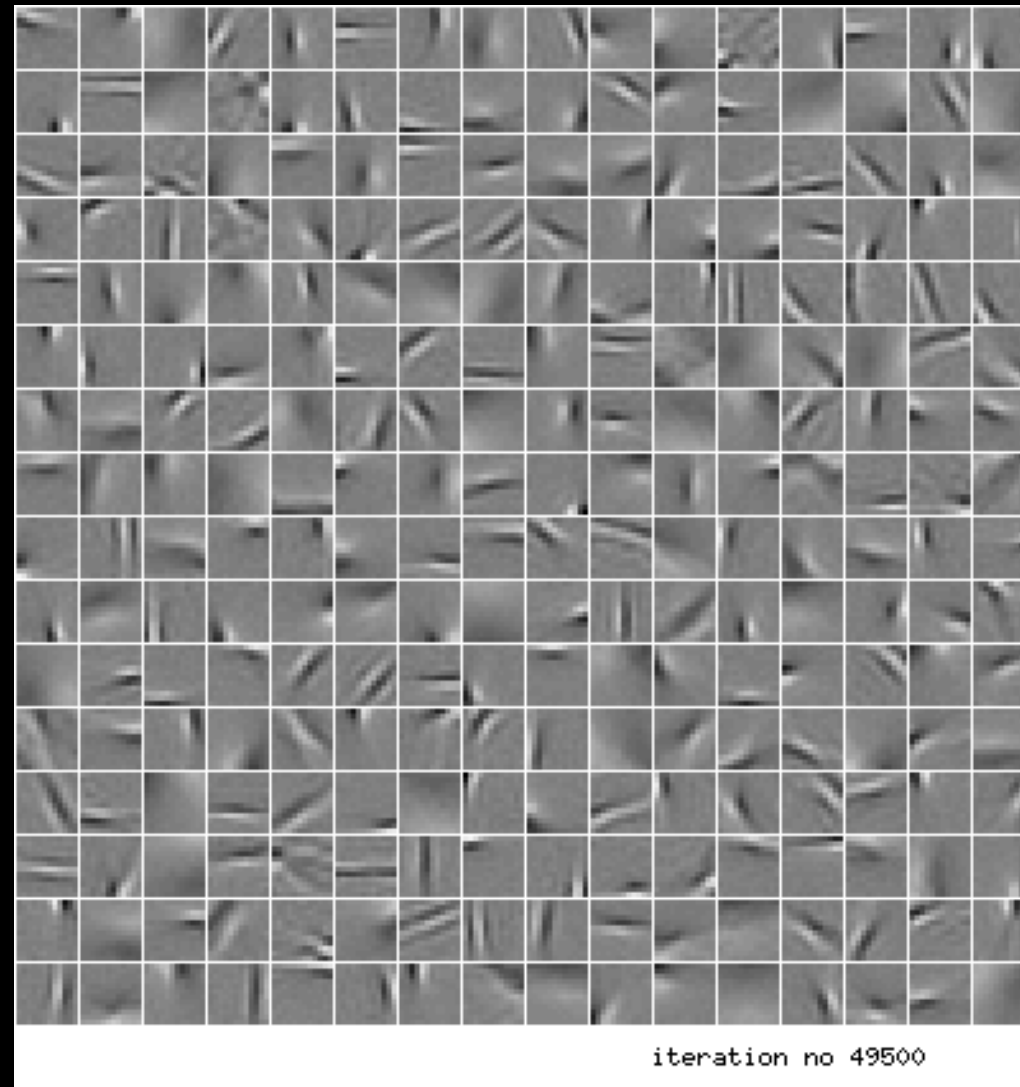


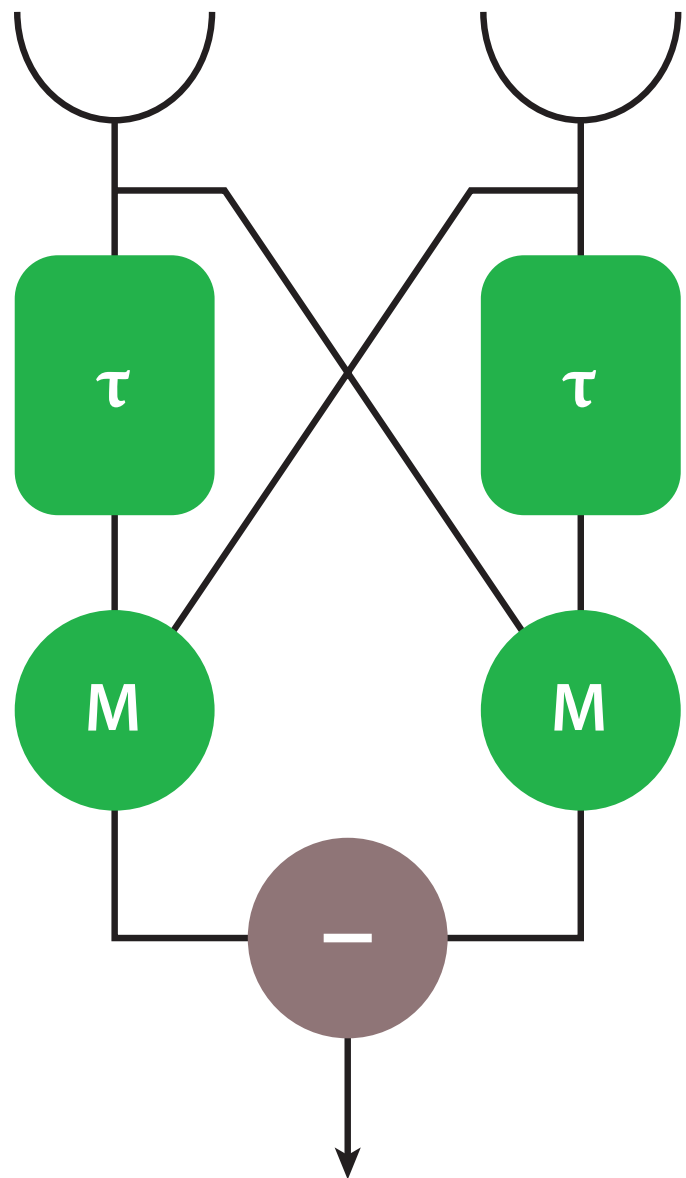
Figure 2.14 Temporal structure of a receptive field. The function $D_t(\tau)$ of equation 2.29 with $\alpha = 1/(15 \text{ ms})$.

Convolutional neural net (CNN) was inspired by information processing in human visual pathway

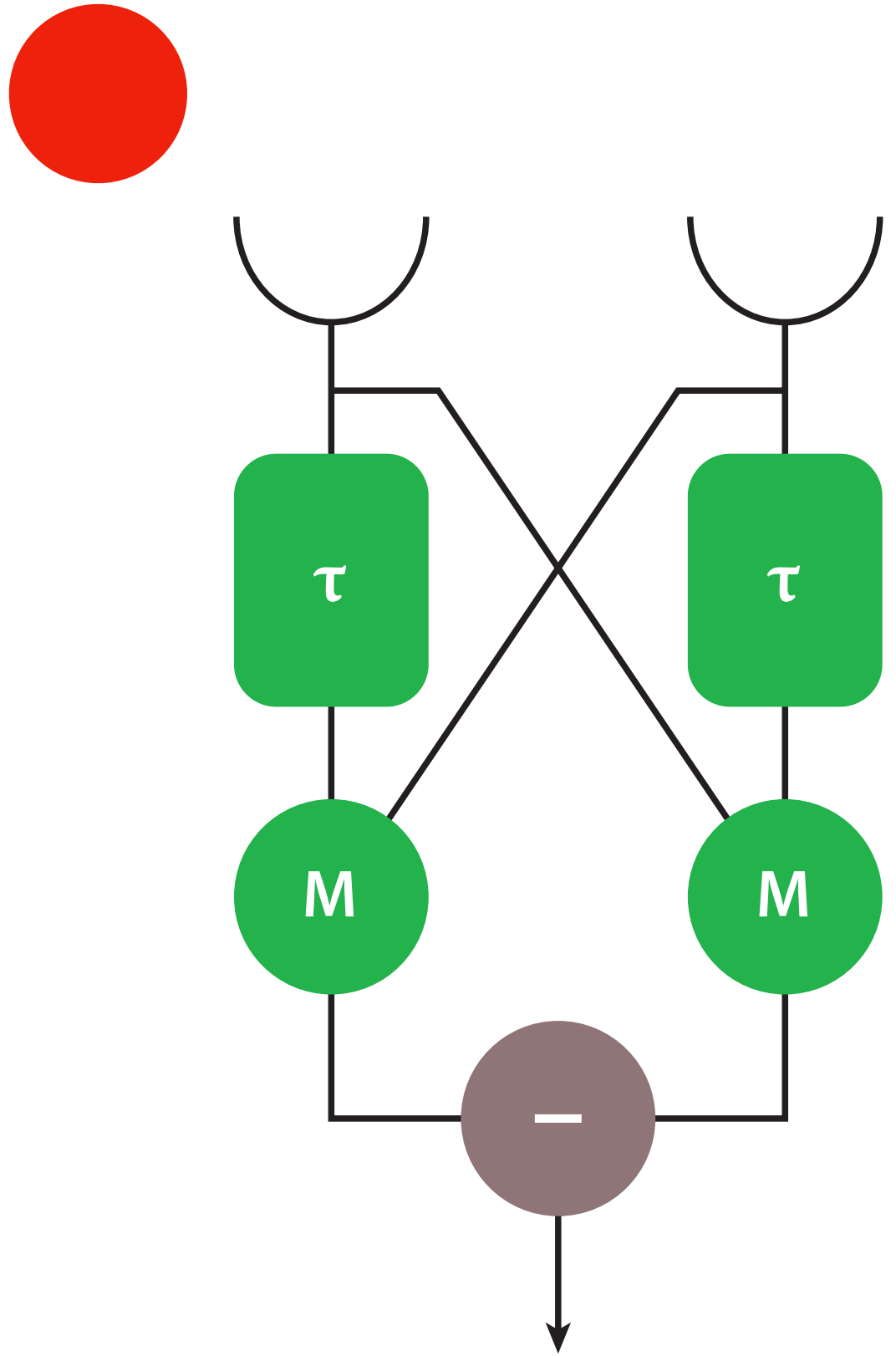


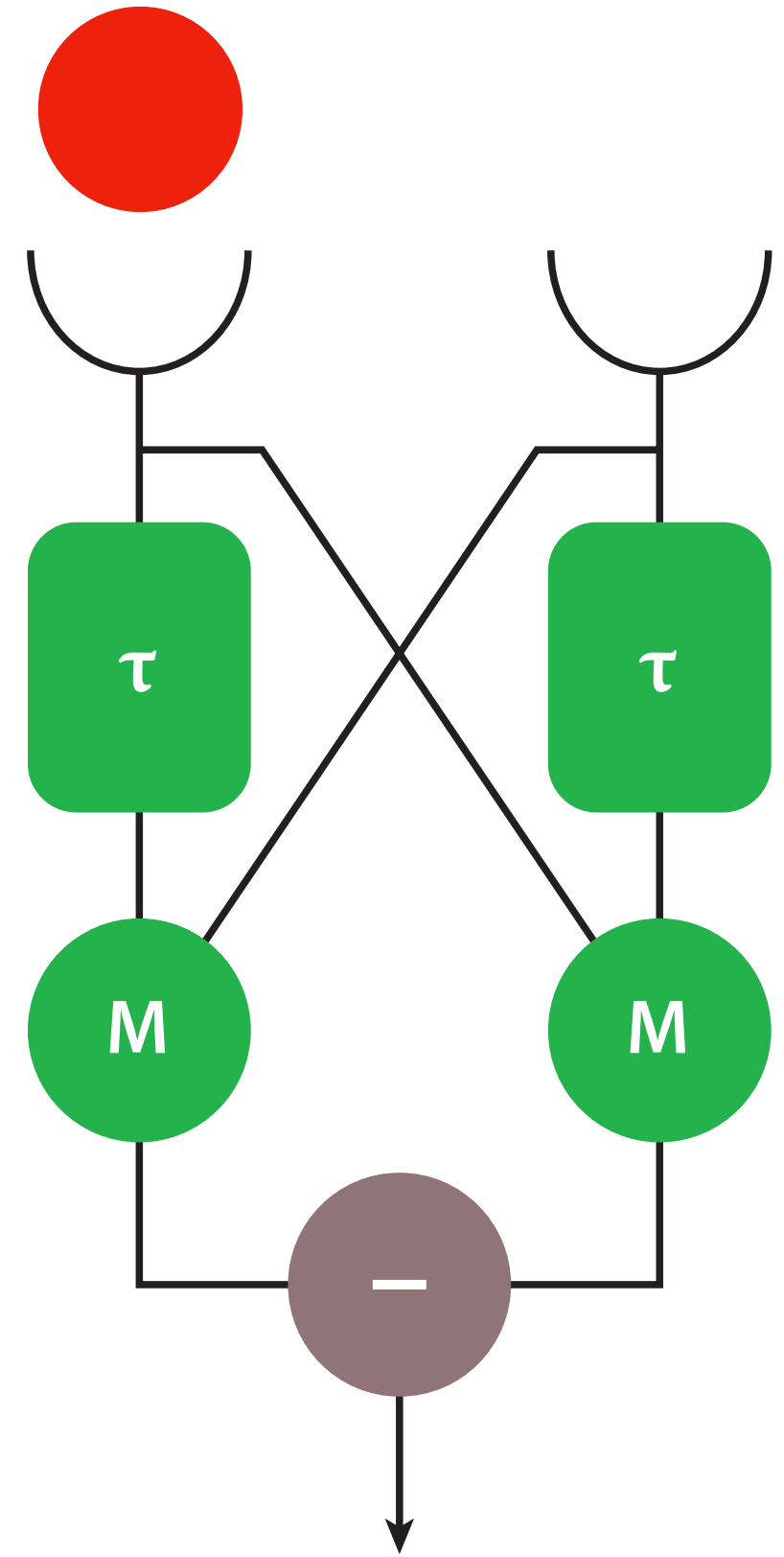
In the first layer of CNN, neurons can generate receptive field just like simple cells in visual cortex

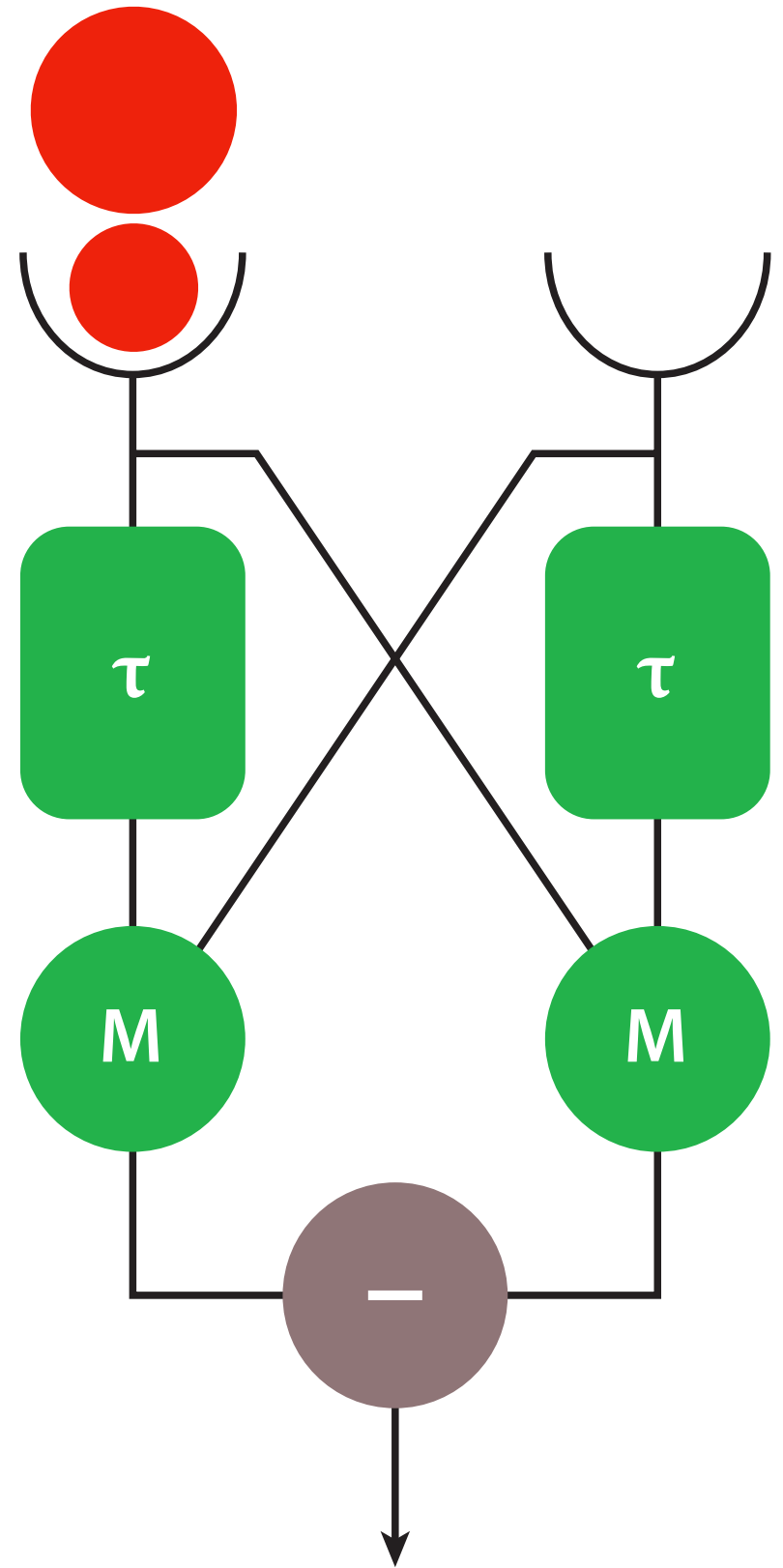
Hassenstein-Reichardt Detector Model

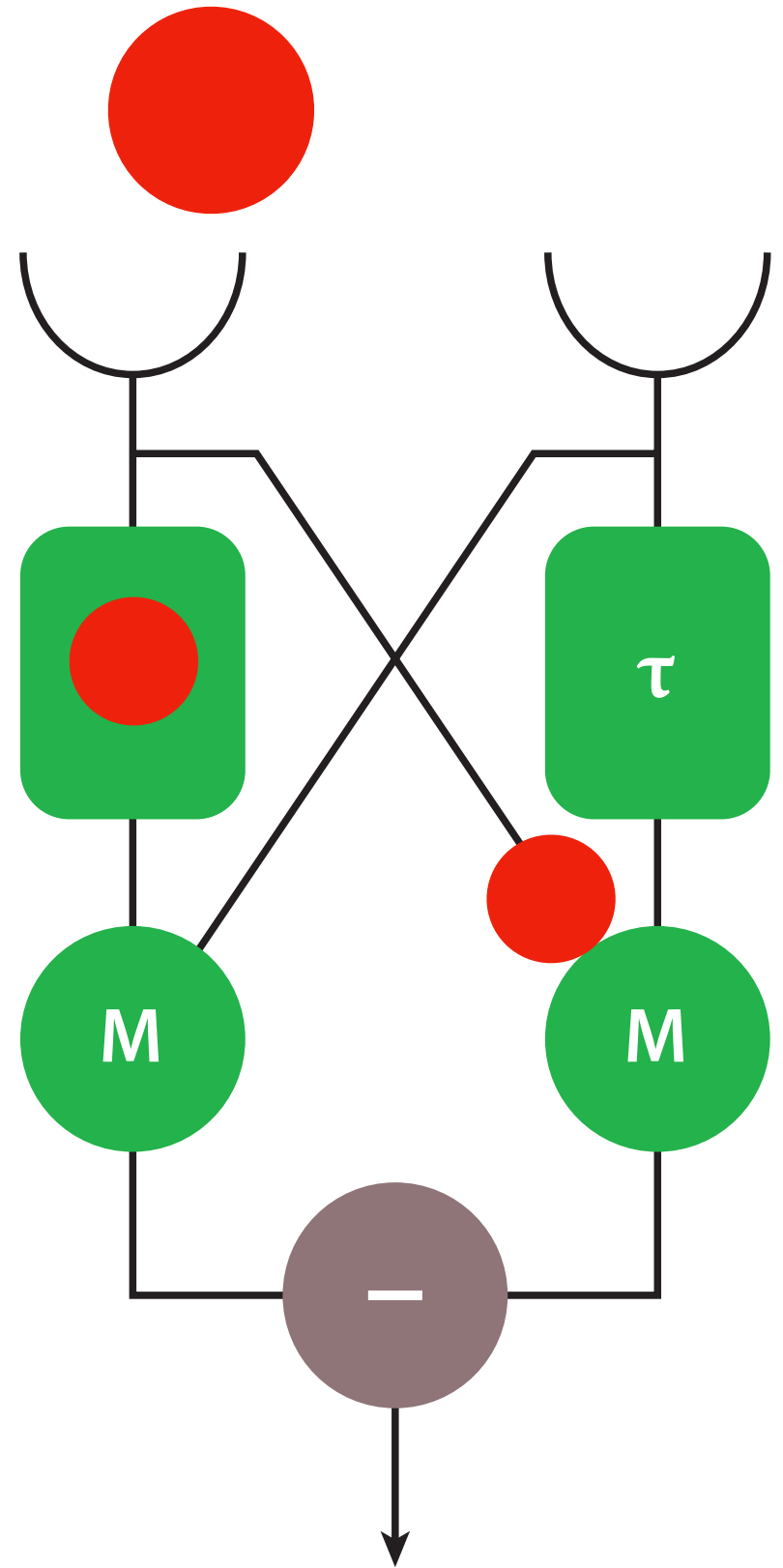


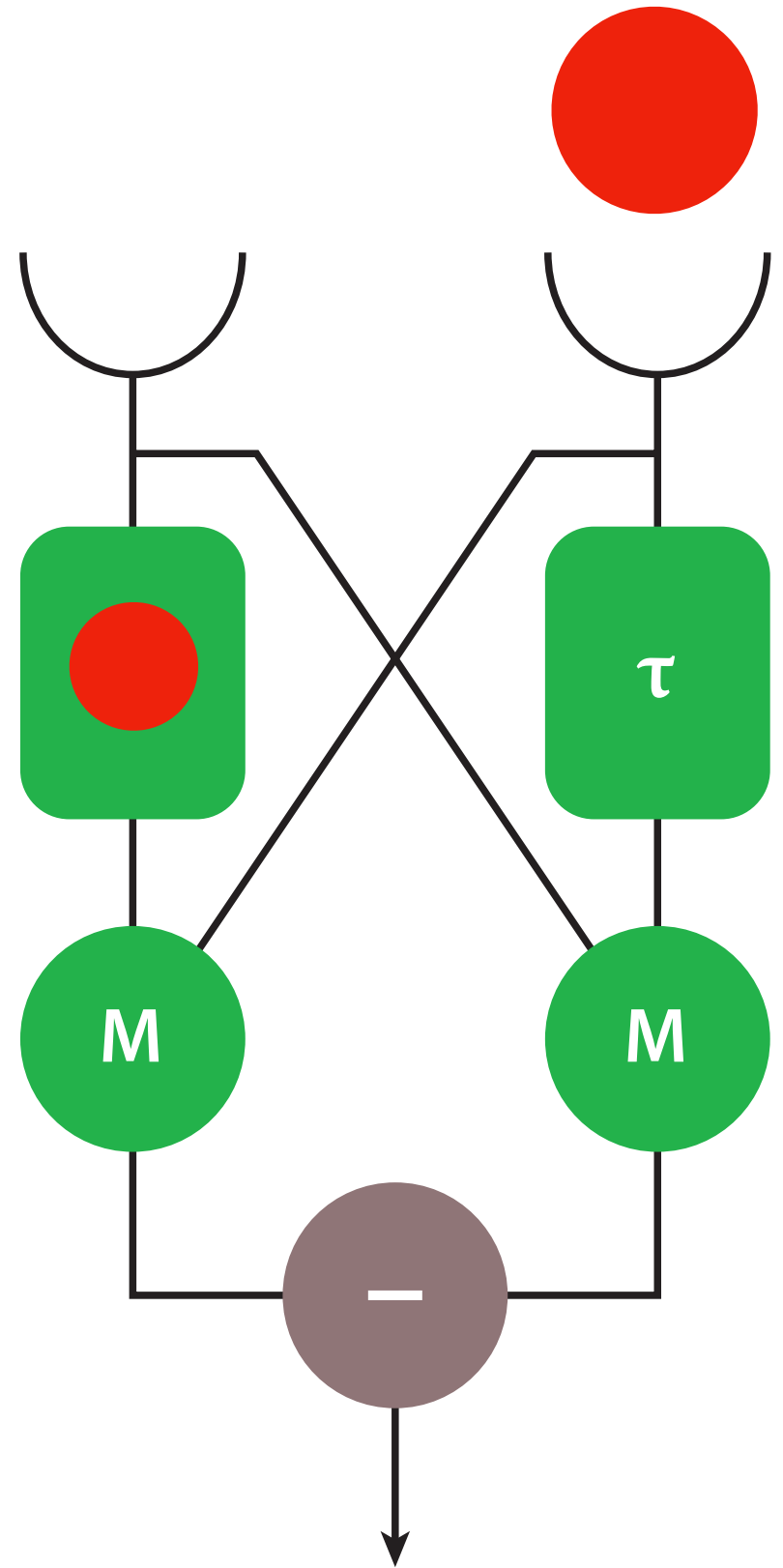
Werner Reichardt

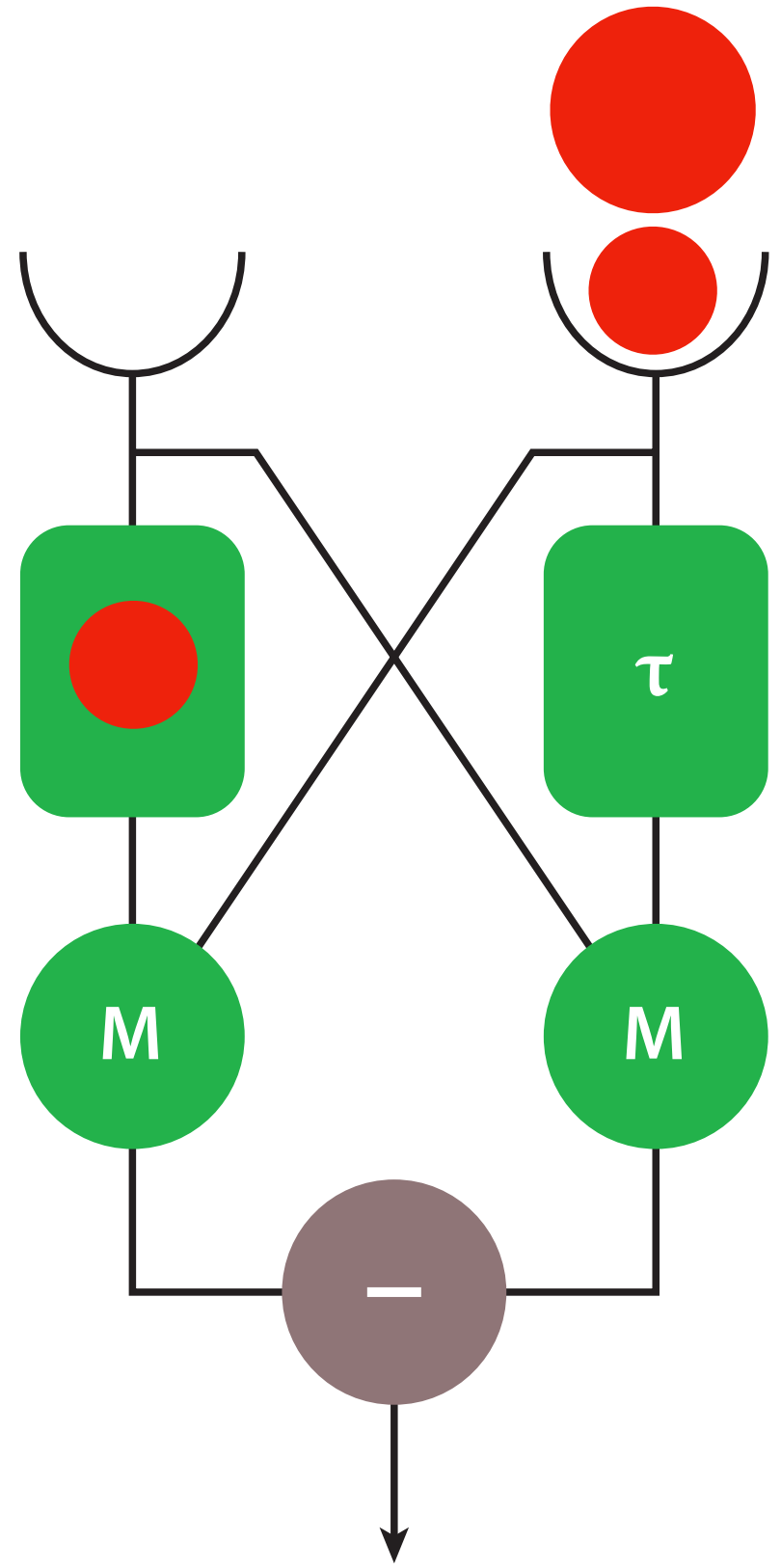


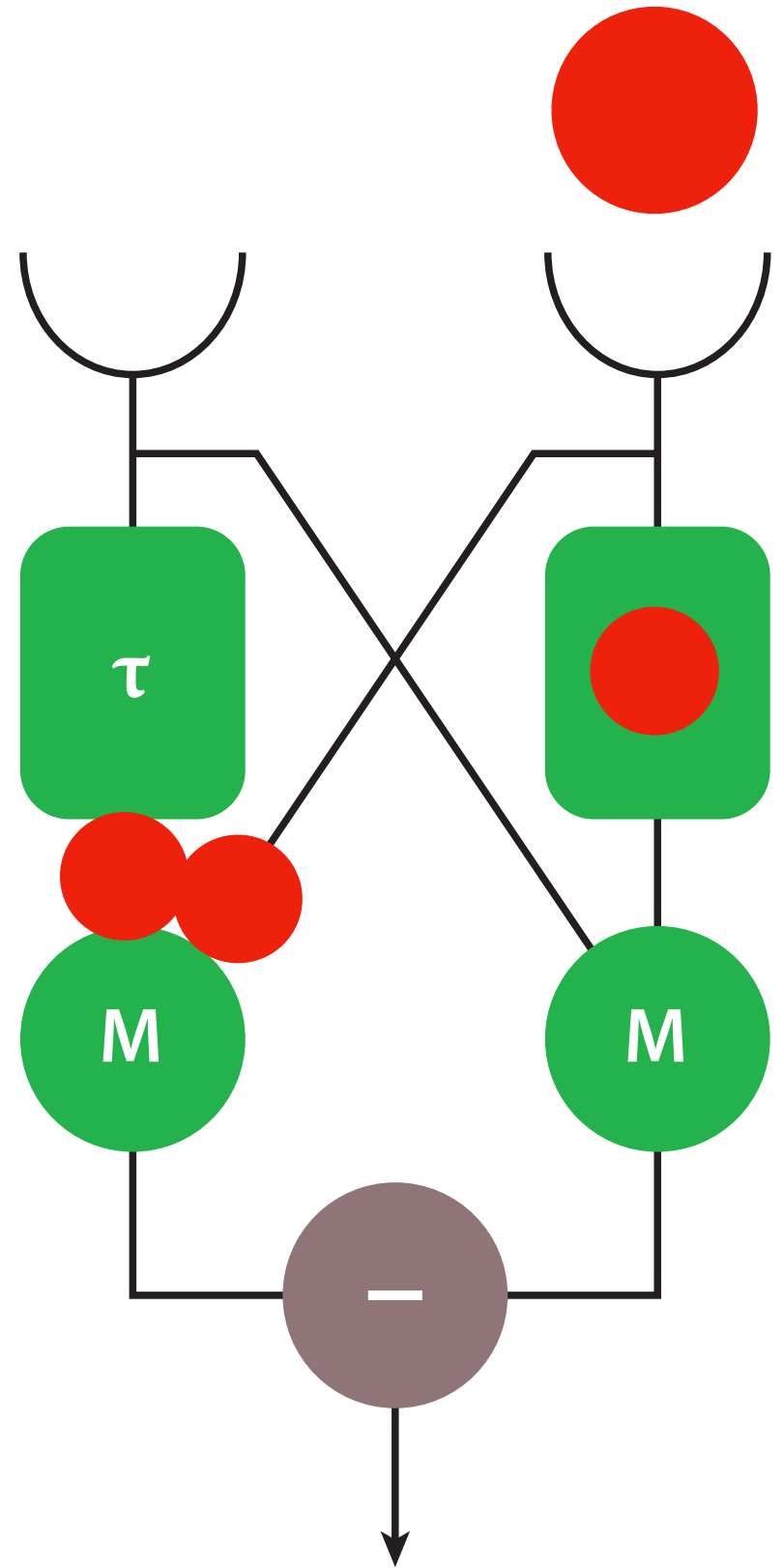


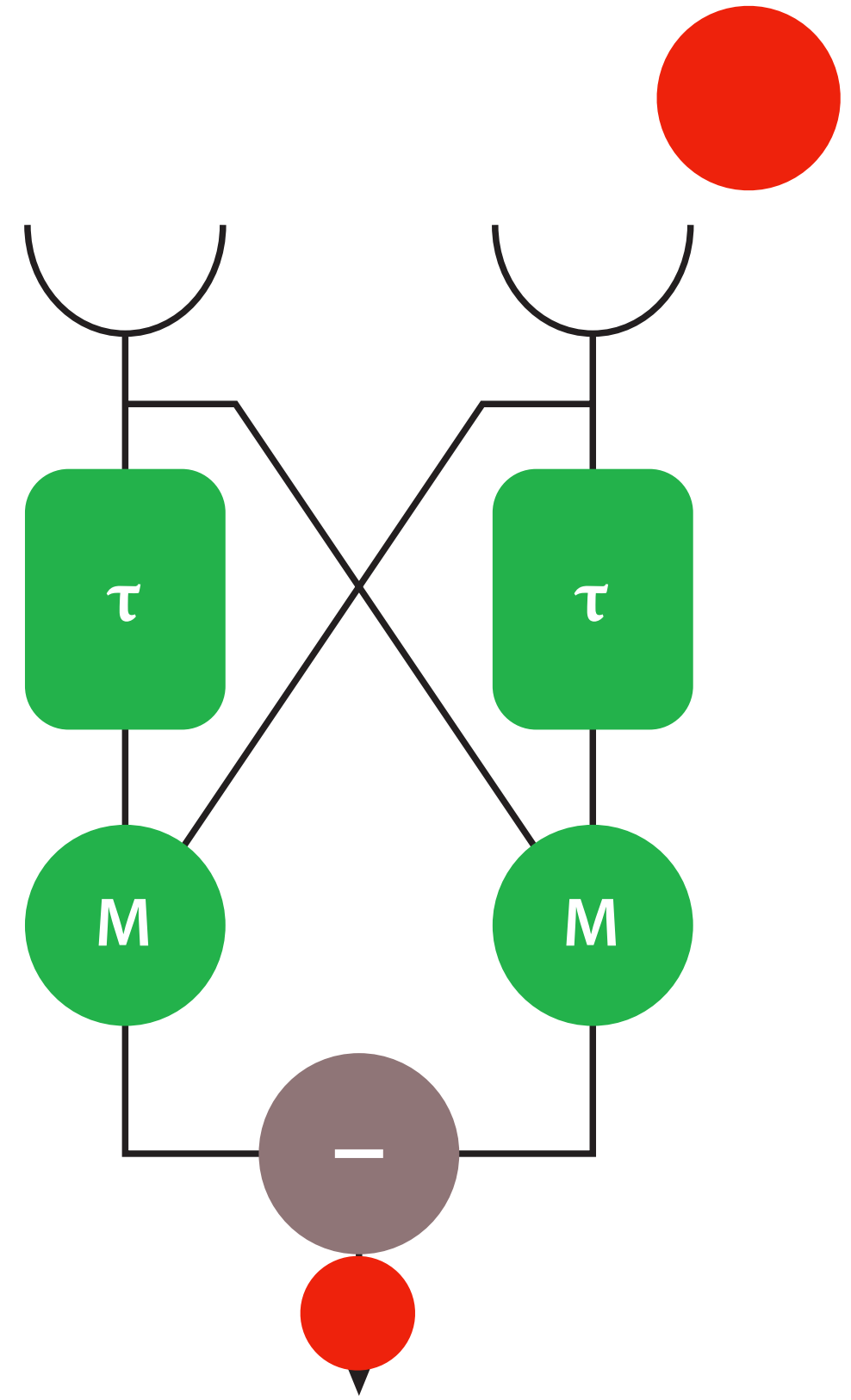




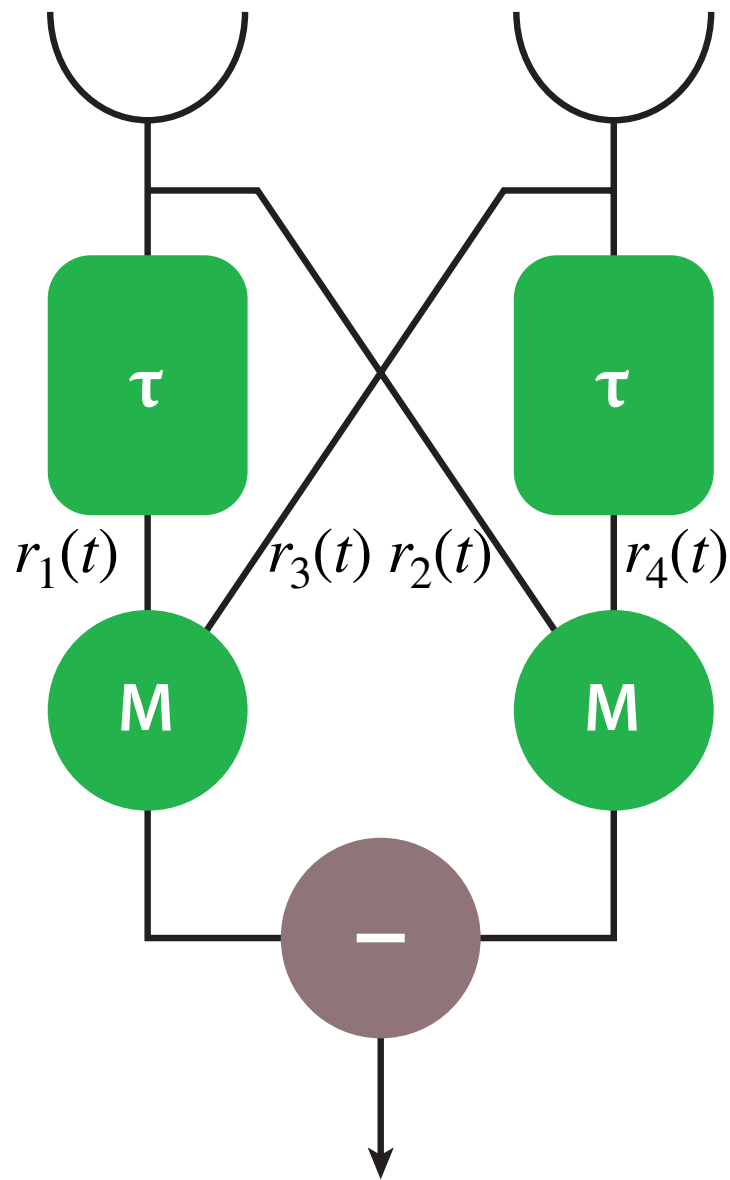








Hassenstein-Reichardt Detector Model



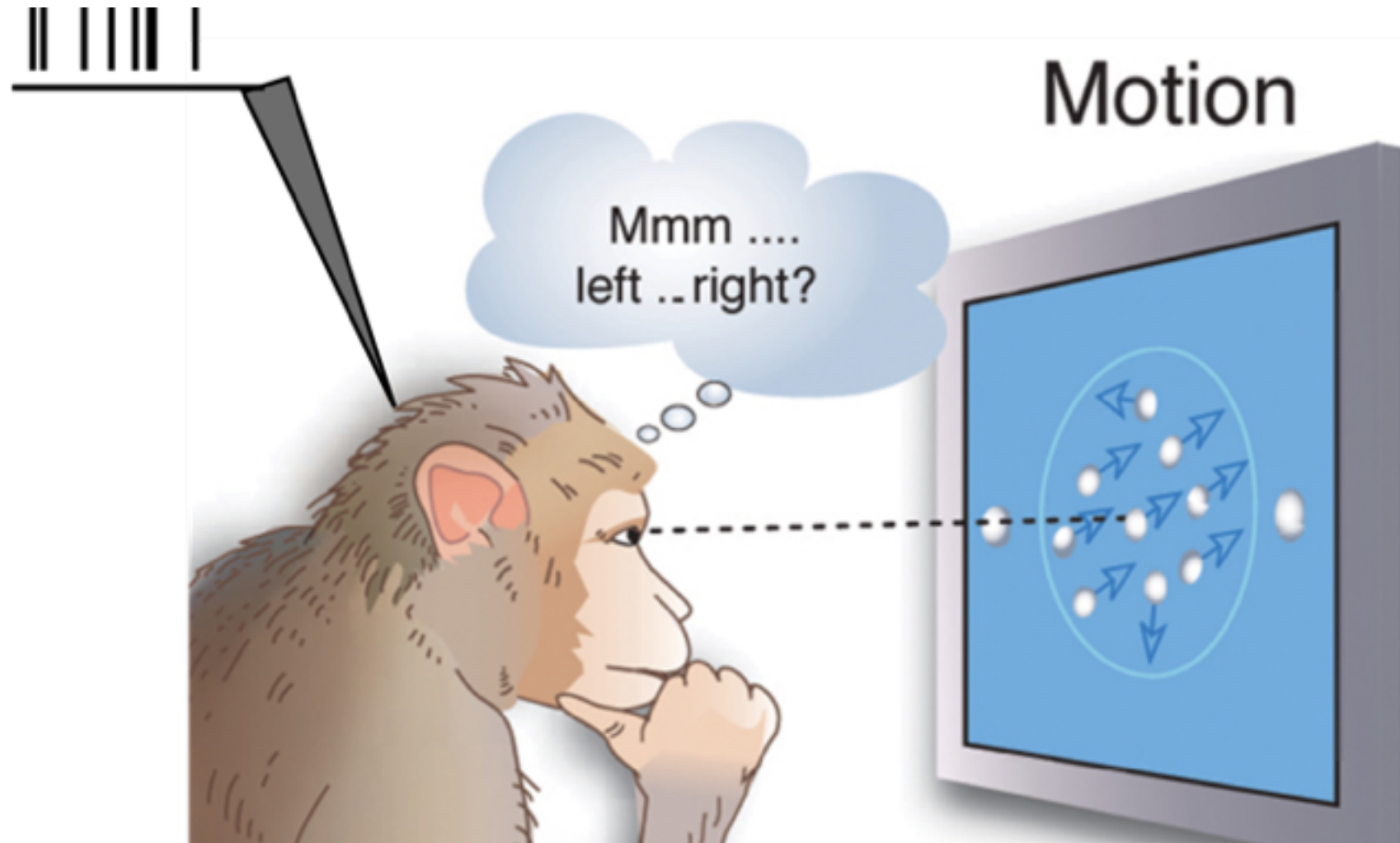
$$r_1(t) = \int_0^{\infty} s_1(t - \tau) D(\tau) d\tau; \quad r_2(t) = \int_0^{\infty} s_1(t - \tau) \delta(\tau) d\tau$$
$$r_3(t) = \int_0^{\infty} s_2(t - \tau) \delta(\tau) d\tau; \quad r_4(t) = \int_0^{\infty} s_2(t - \tau) D(\tau) d\tau;$$
$$R(t) = r_1(t)r_3(t) - r_2(t)r_4(t)$$

$$D(\tau) = \frac{1}{\tau_0} \exp(-\tau/\tau_0)$$

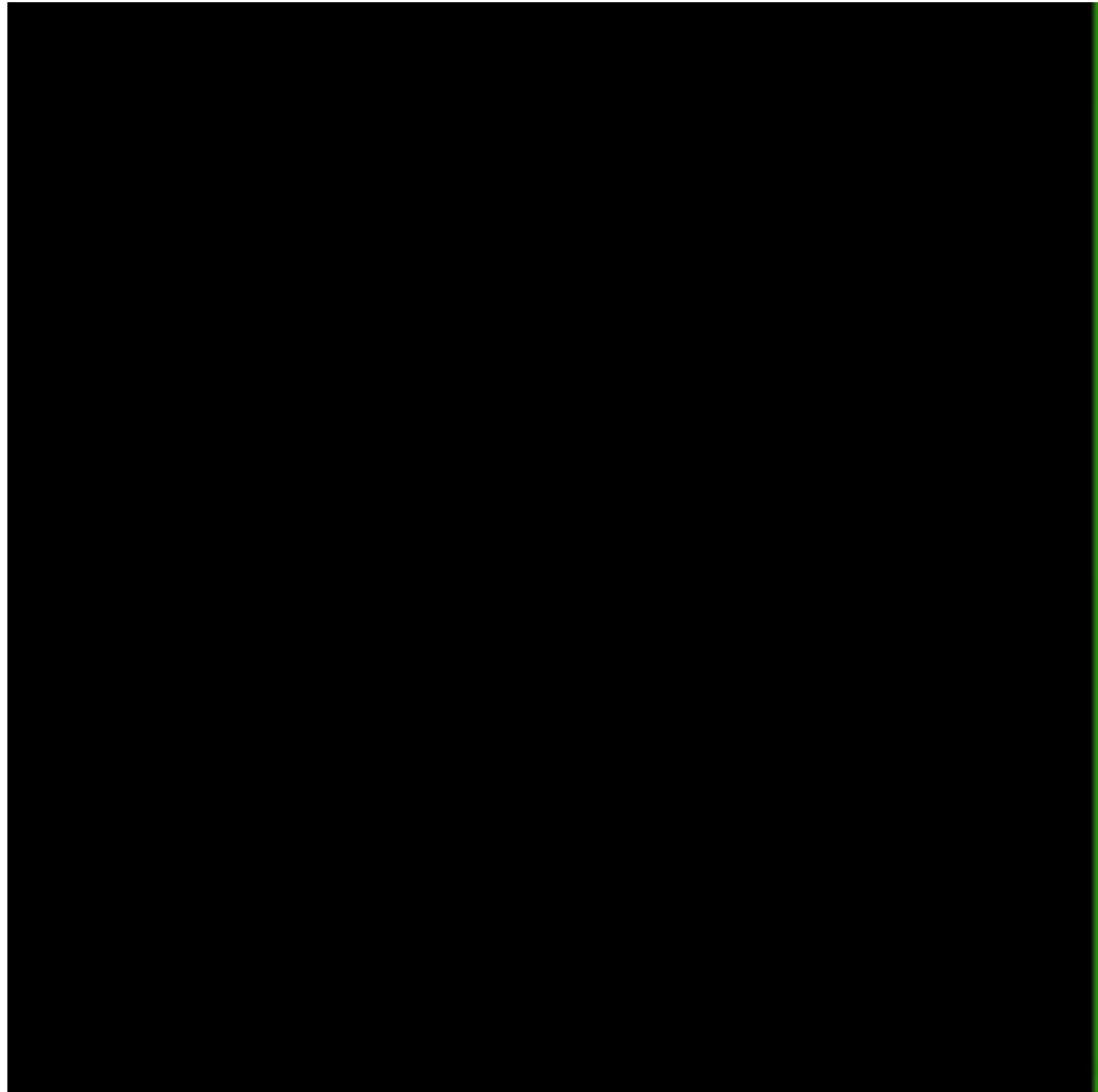
$$\langle R \rangle = \frac{\omega \tau_0}{\omega^2 \tau_0^2 + 1}$$

Neuron Decoding

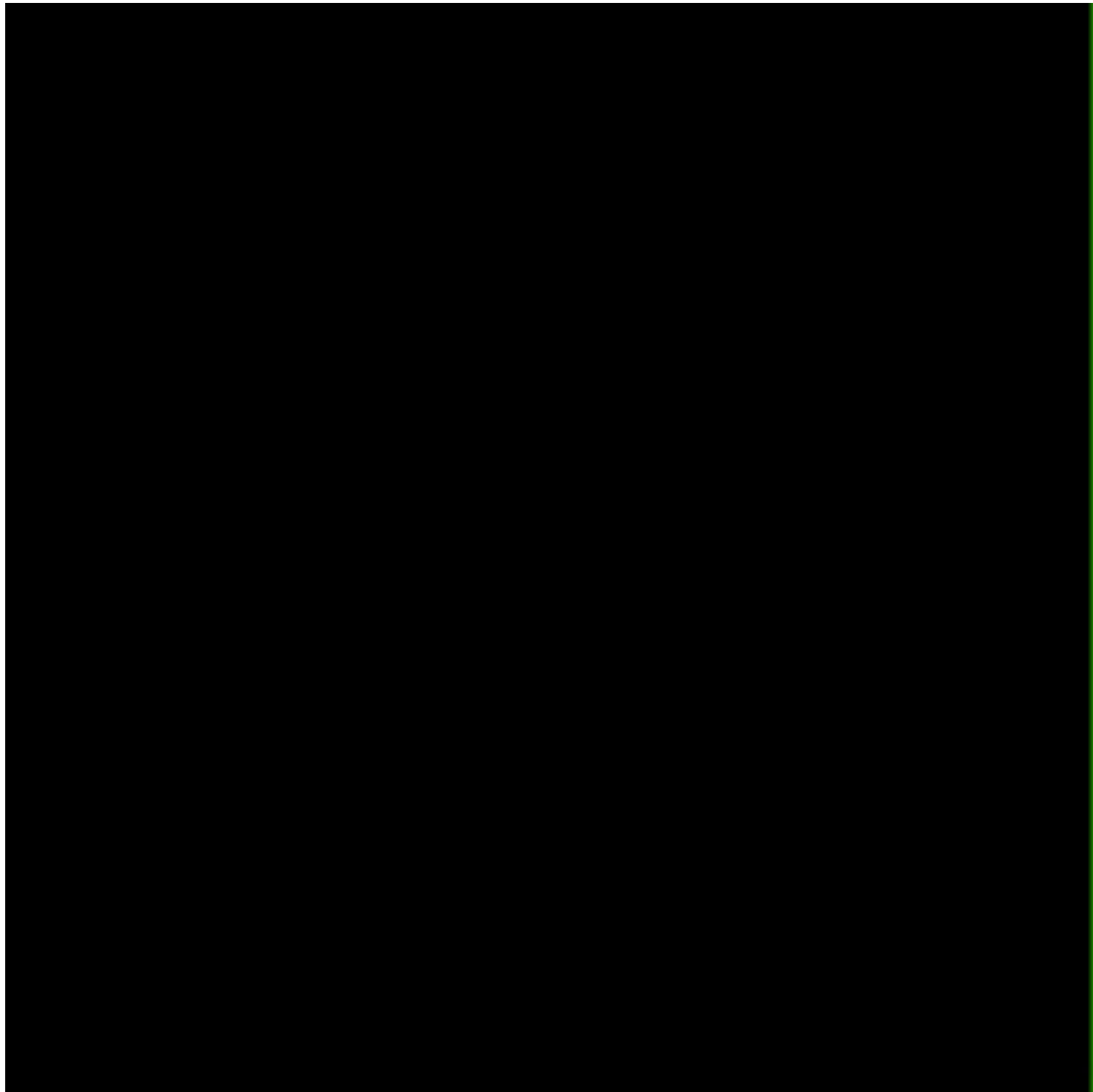
Random dots motion discrimination task



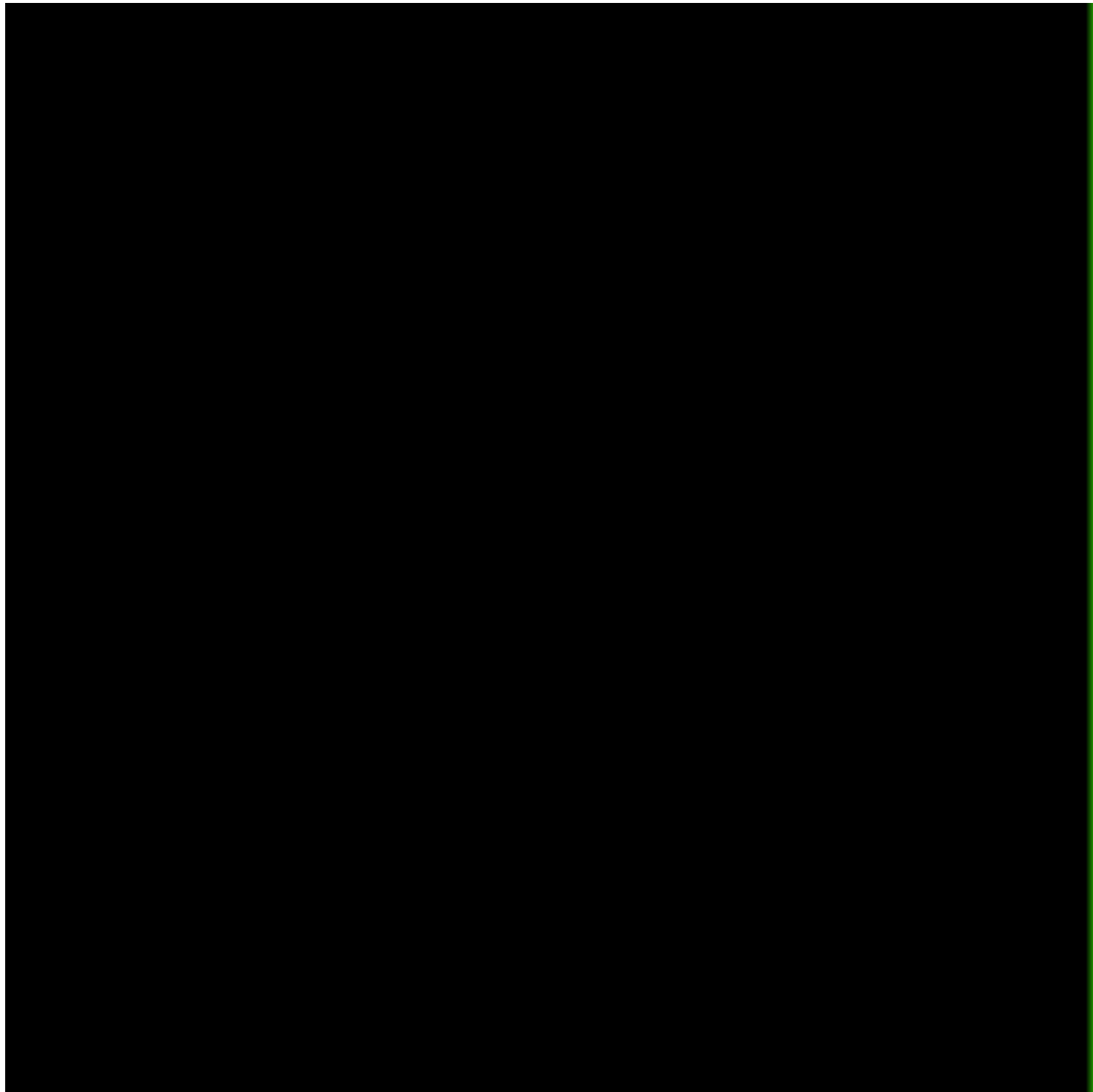
This slide and the following movies are adapted from Professor Tianming Yang's lectures



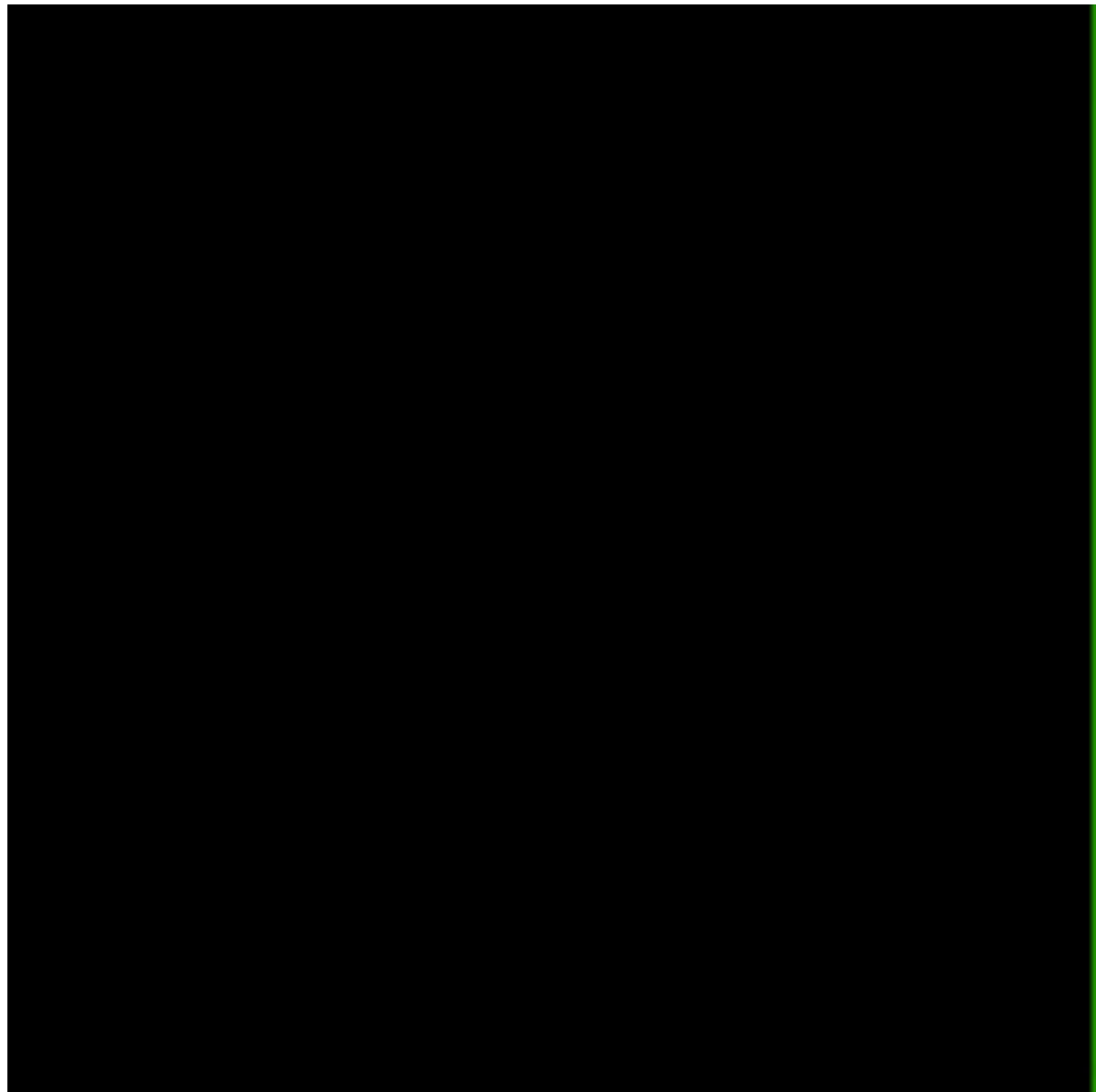
← 100%



51.2%

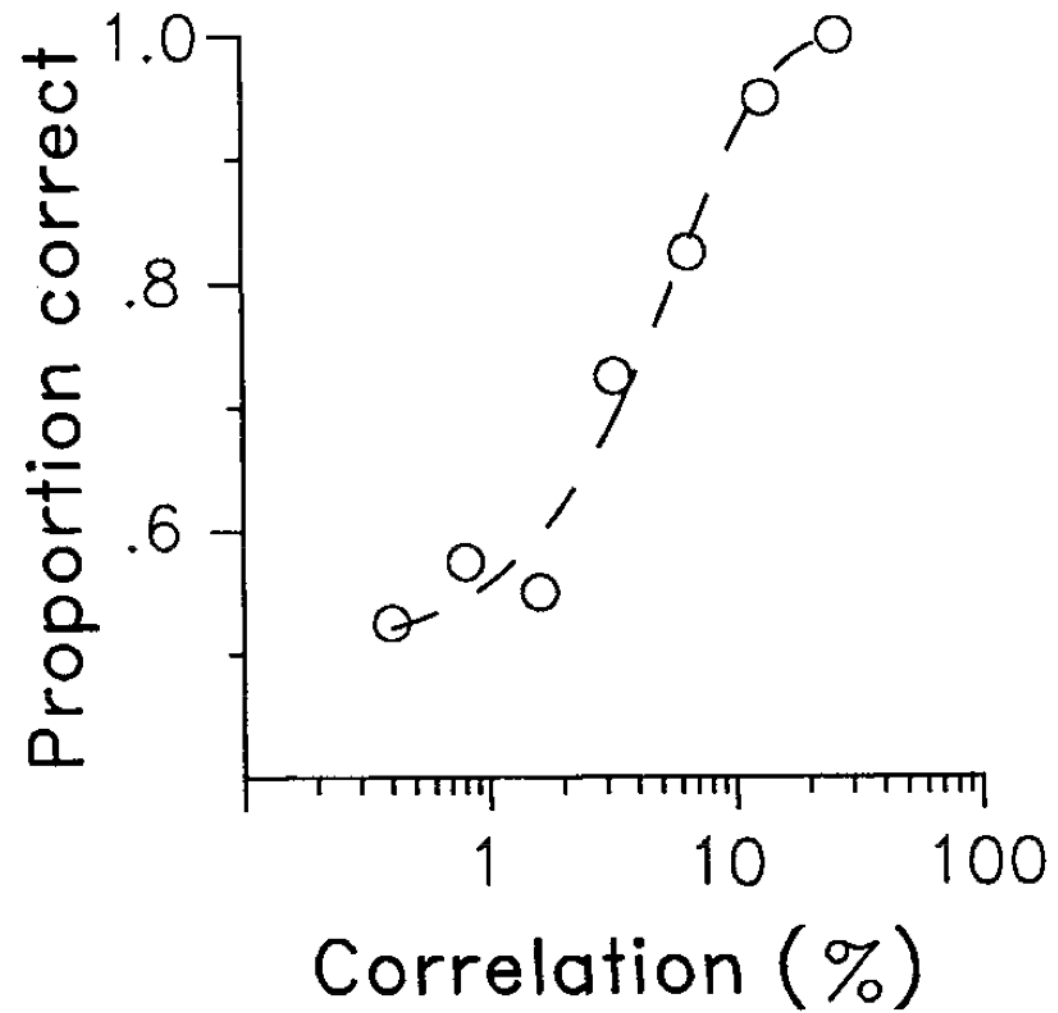


12.8%



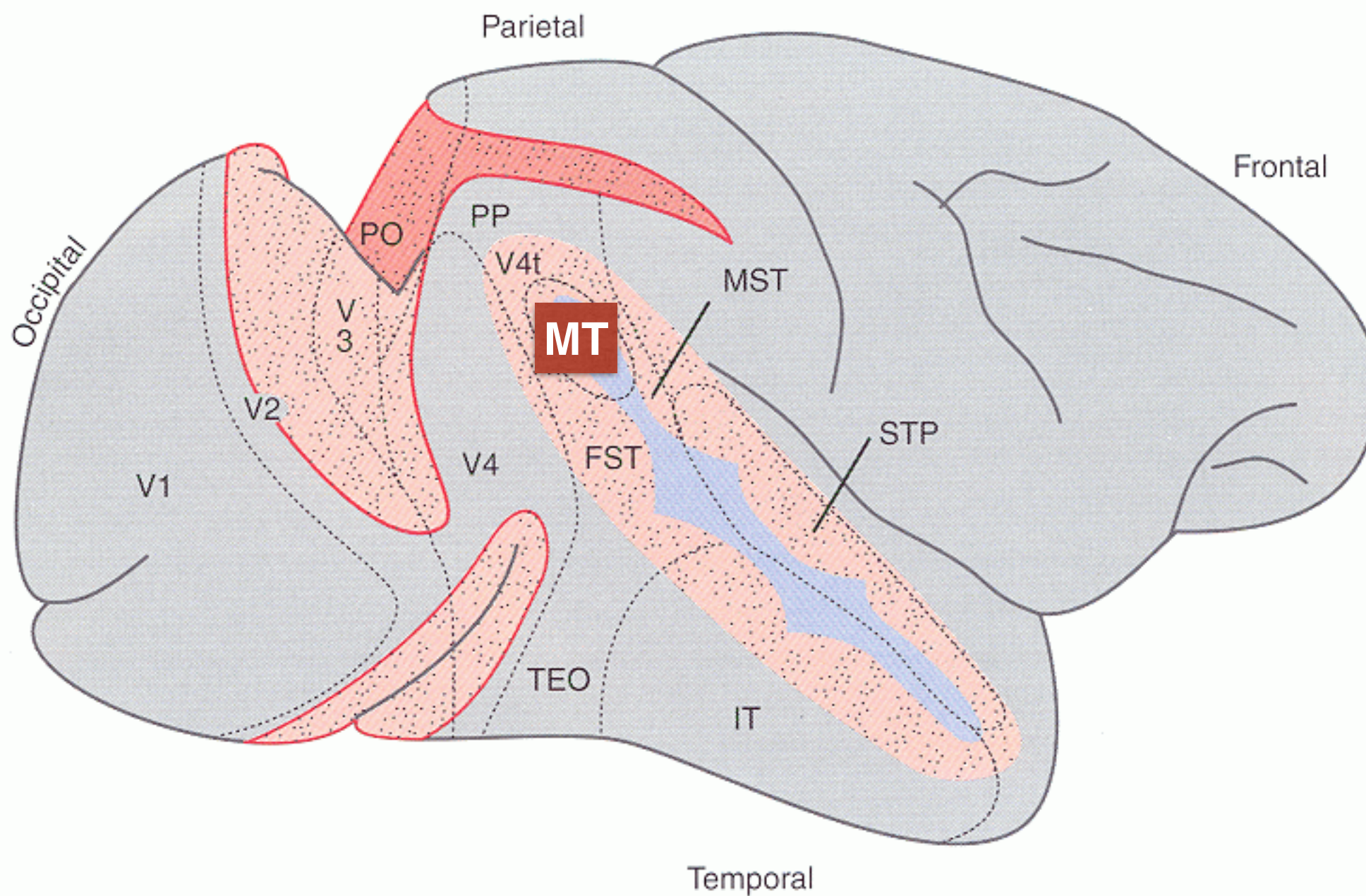
0%

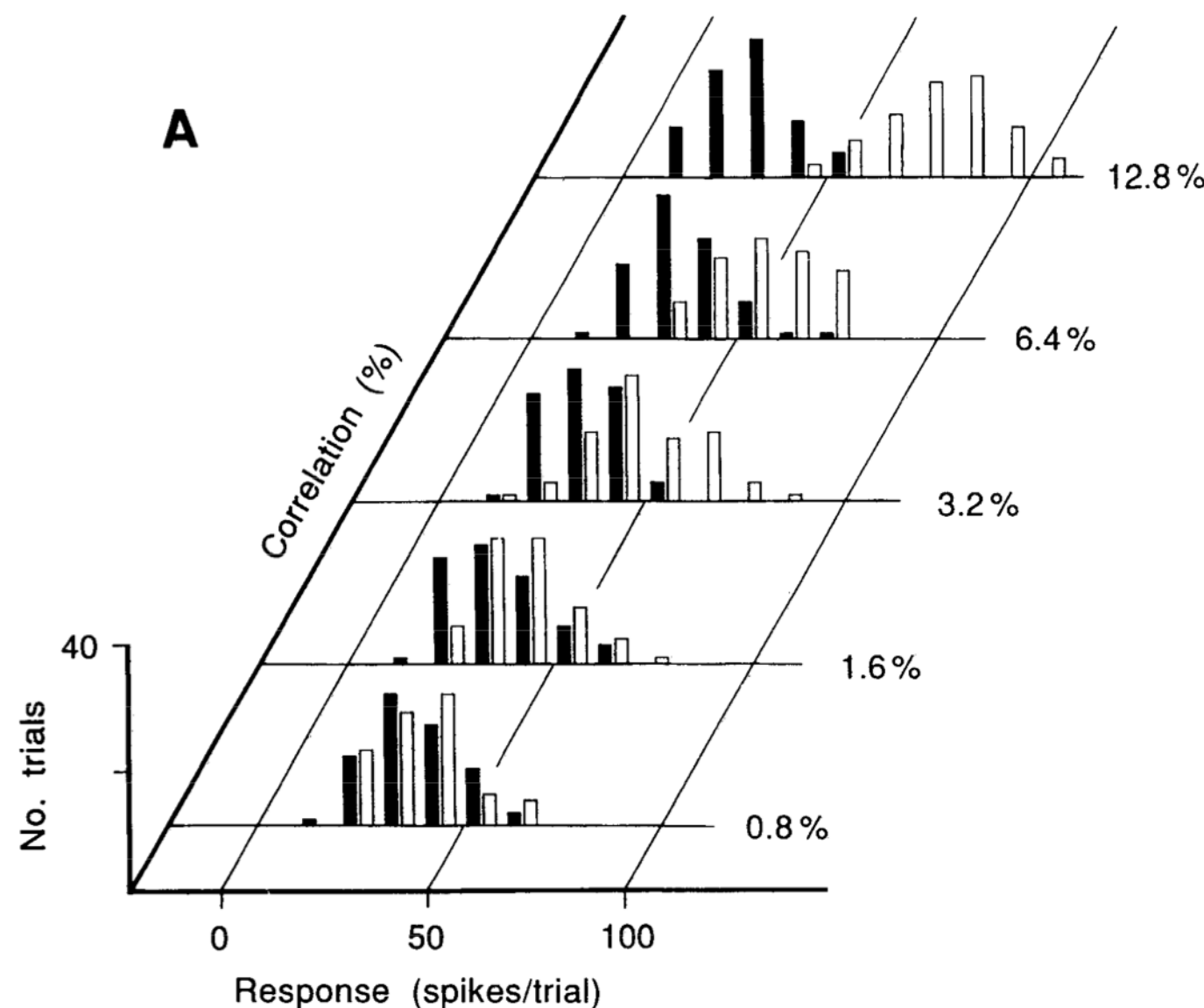
Behavior Performance



Britten, Shadlen, Newsome and Movshon, J Neurosci., 1992

Measuring neural activity in MT

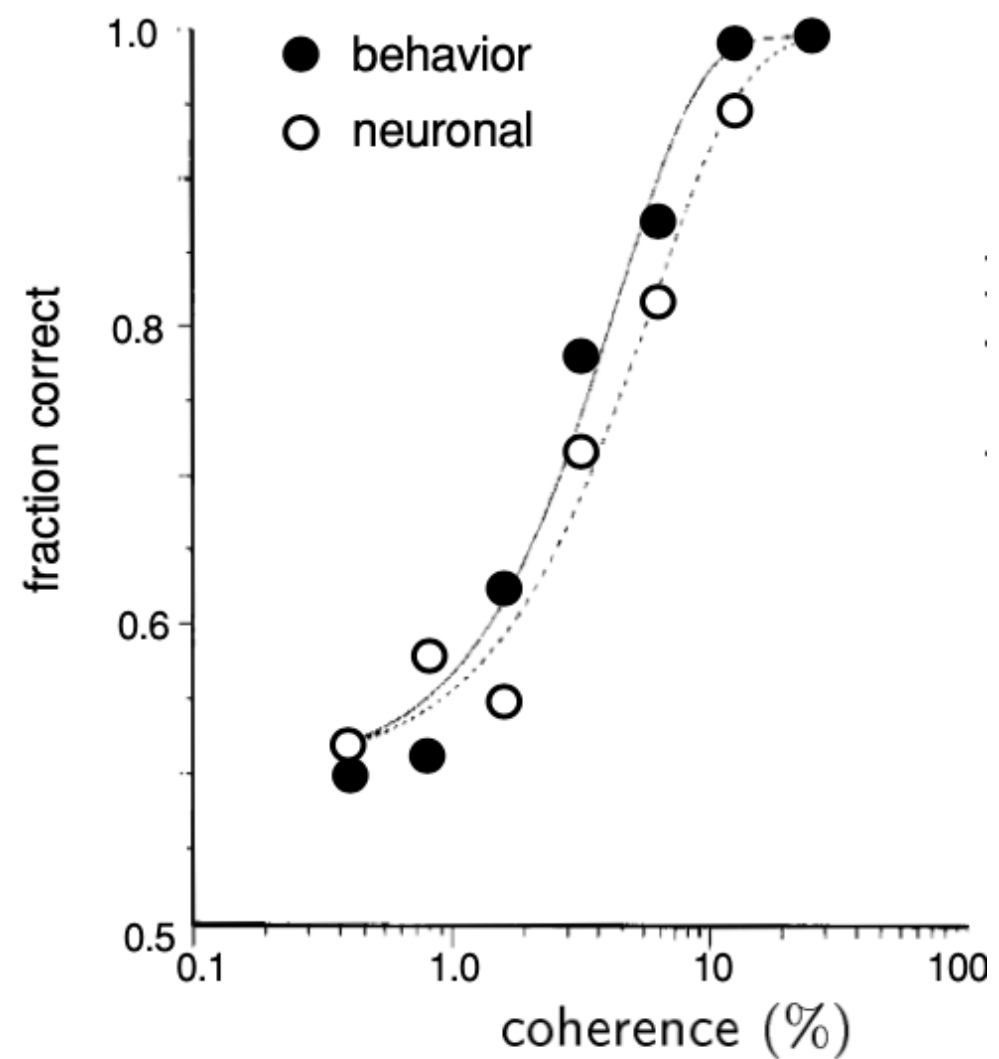




$$d = \frac{\langle r \rangle_+ - \langle r \rangle_-}{\sigma}$$

$$P(\text{correct}) = \frac{1}{\sqrt{\pi}} \int_{-d/2}^{\infty} dx \exp(-x^2)$$

Neural Correlates with Behavior

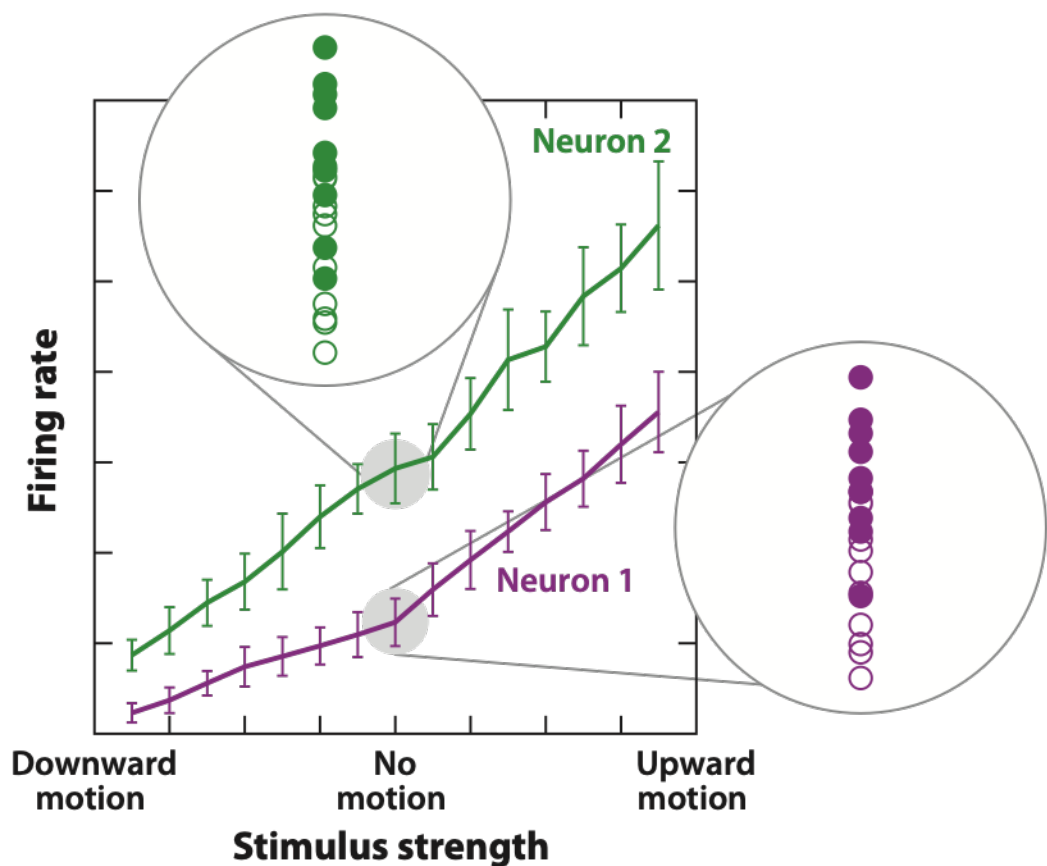


Population decoding

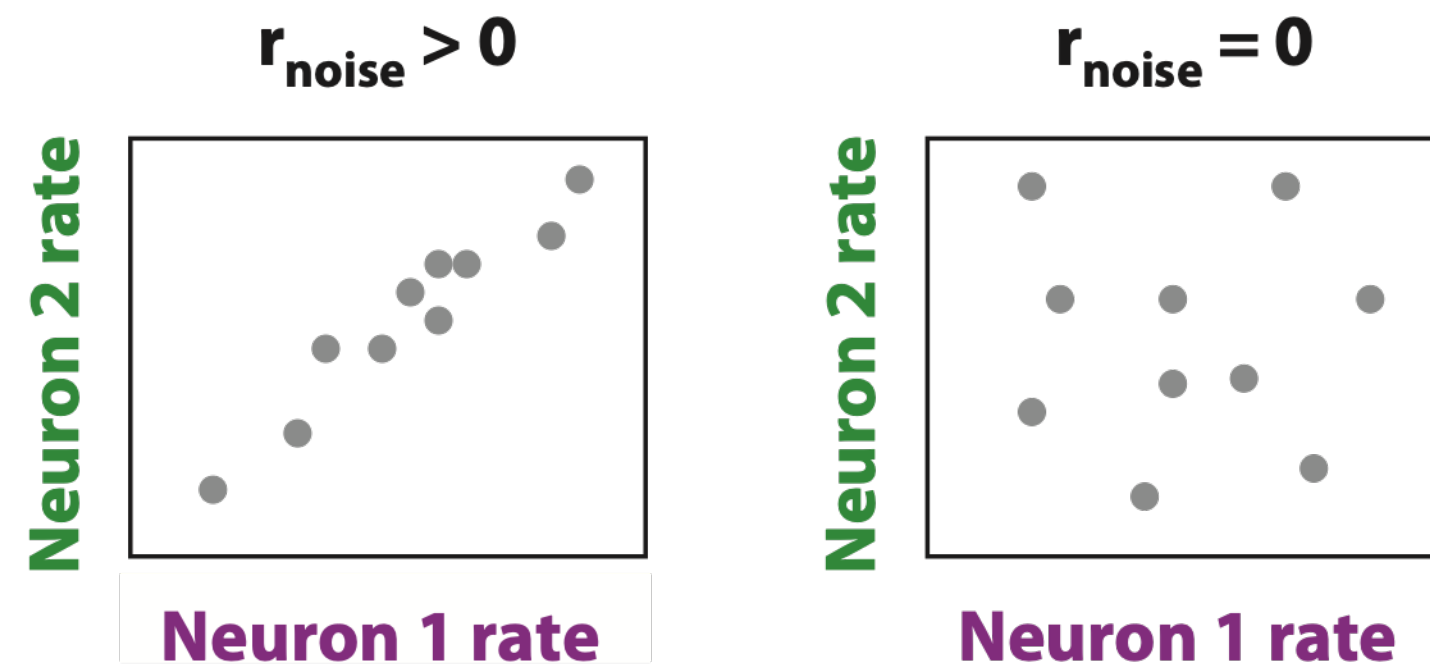
$$k_+ = \sum_{i=1}^N r_+^i \quad k_- = \sum_{i=1}^N r_-^i$$

$$d^2 = \frac{\left(\langle k_+ \rangle - \langle k_- \rangle\right)^2}{\langle \left(k_+ - \langle k_+ \rangle\right)^2 \rangle}$$

Population decoding with correlated neurons

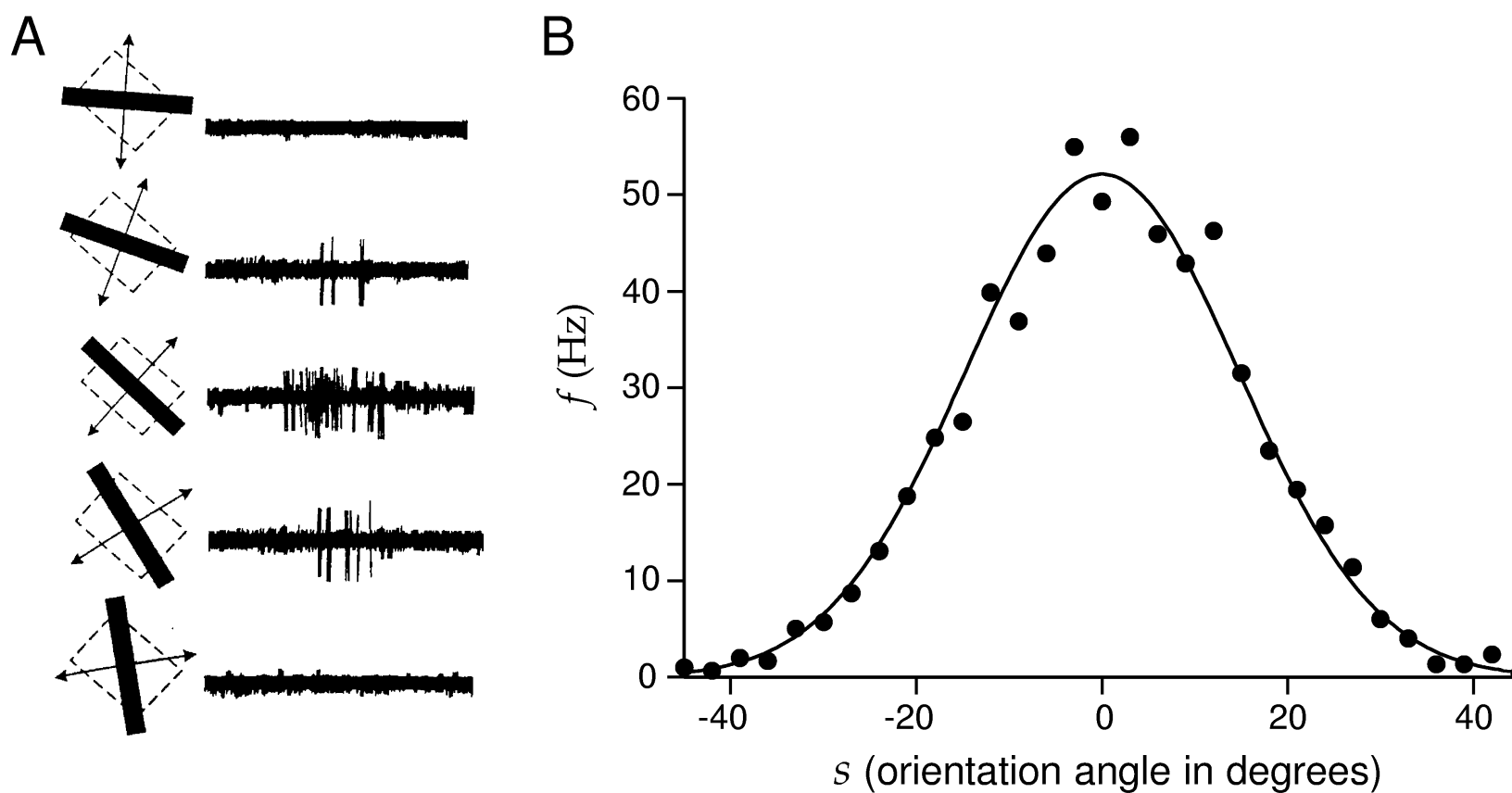


Signal Correlation



Noise Correlation

Orientation selectivity of simple cells in the visual cortex

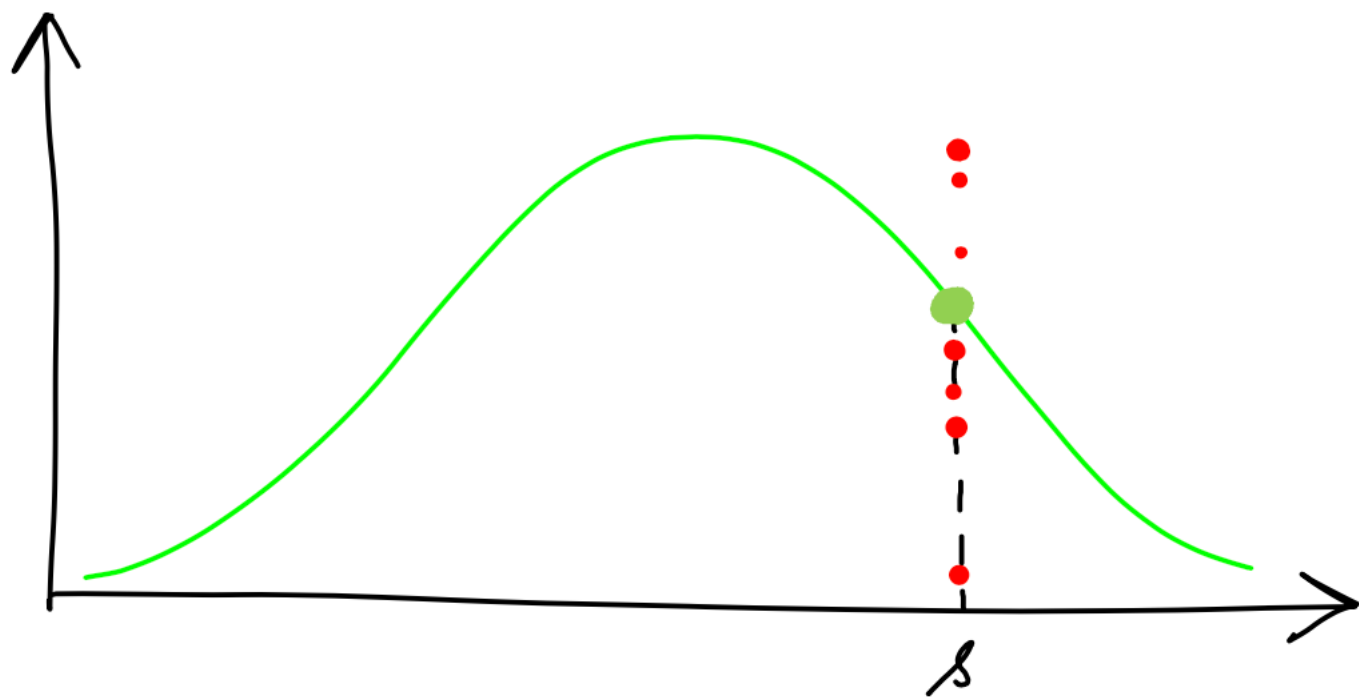


Gaussian tuning curve of a neuron in the primary visual cortex (V1)

Bayesian decoding method

Variability

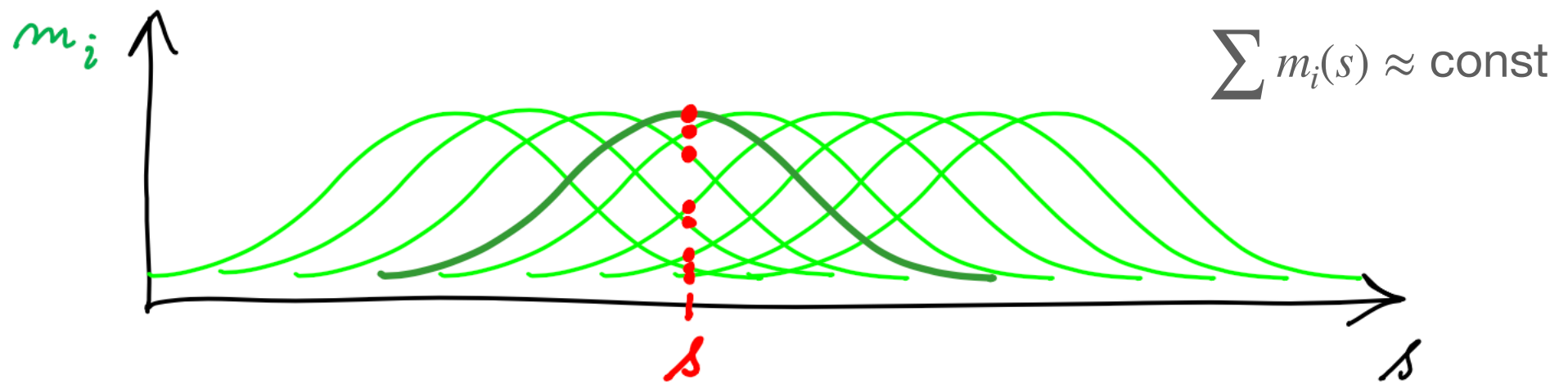
$$r = m(s) + \xi$$



$$p(s|r) = \frac{p(r|s)p(s)}{p(r)}$$

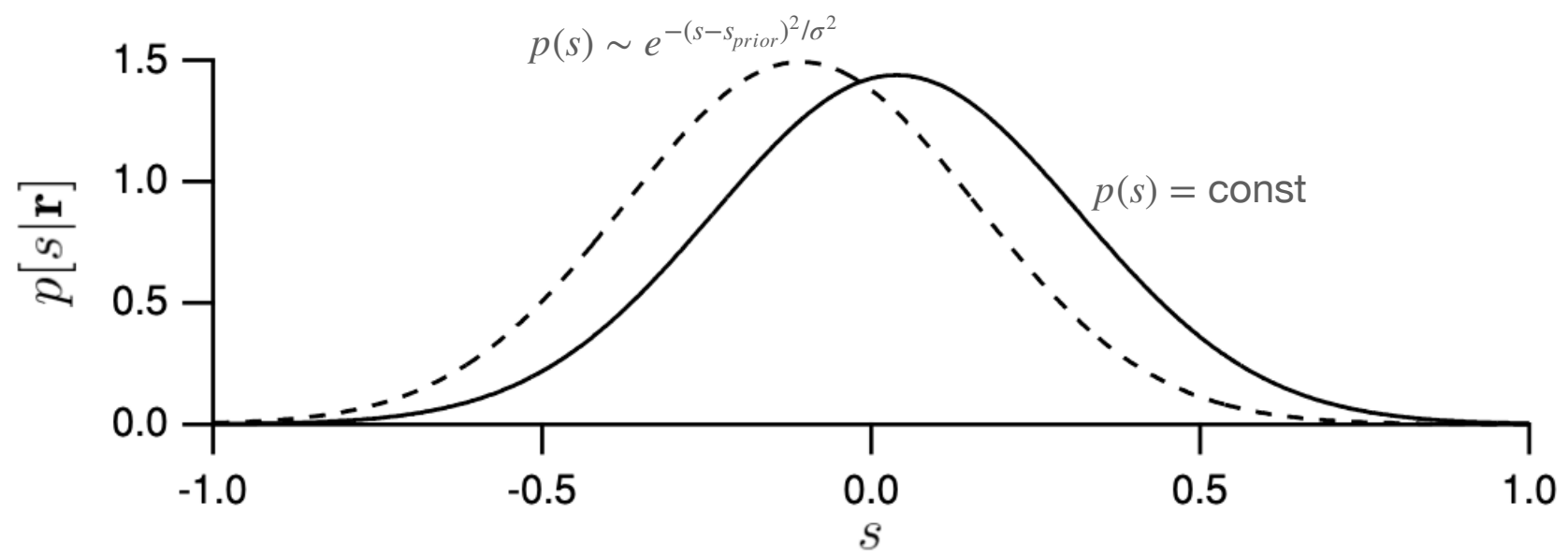
Likelihood Prior
Normalization factor

Population decoding



$$p(n_i | s) = \frac{[m_i(s)T]^{n_i}}{n_i!} \exp(-m_i(s)T)$$

$$p(\mathbf{r} | s) = \prod_{i=1}^N p(n_i | s)$$



$$s - \langle s_{est} \rangle = b_{est}$$

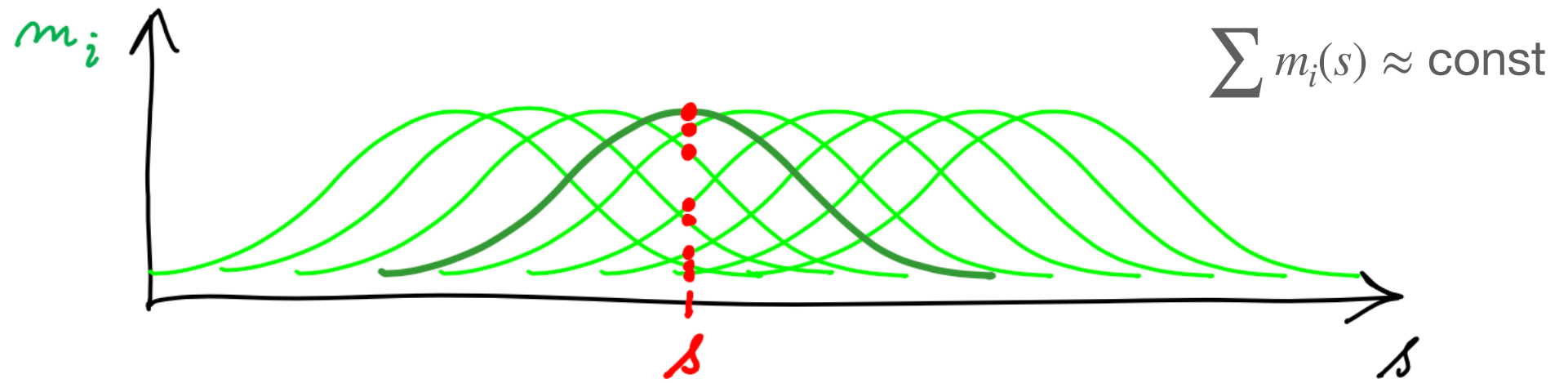
$$\langle (s - s_{est})^2 \rangle = \langle (s - \langle s_{est} \rangle + \langle s_{est} \rangle - s_{est})^2 \rangle = b_{est}^2 + \sigma_{est}^2$$

Cramer-Rao bound and Fisher information

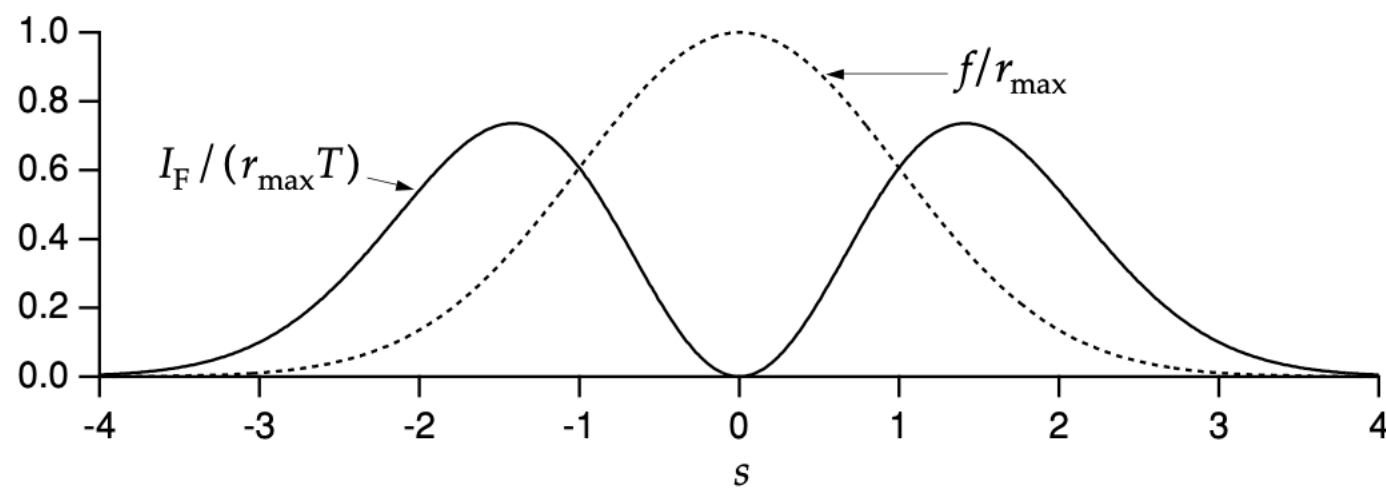
$$\sigma_{est}^2 \geq \frac{(1 + b_{est})^2}{I_F}$$

$$I_F = \left\langle -\frac{\partial^2 \log p(r|s)}{\partial s^2} \right\rangle = - \int dr p(r|s) \frac{\partial^2 \log p(r|s)}{\partial s^2}$$

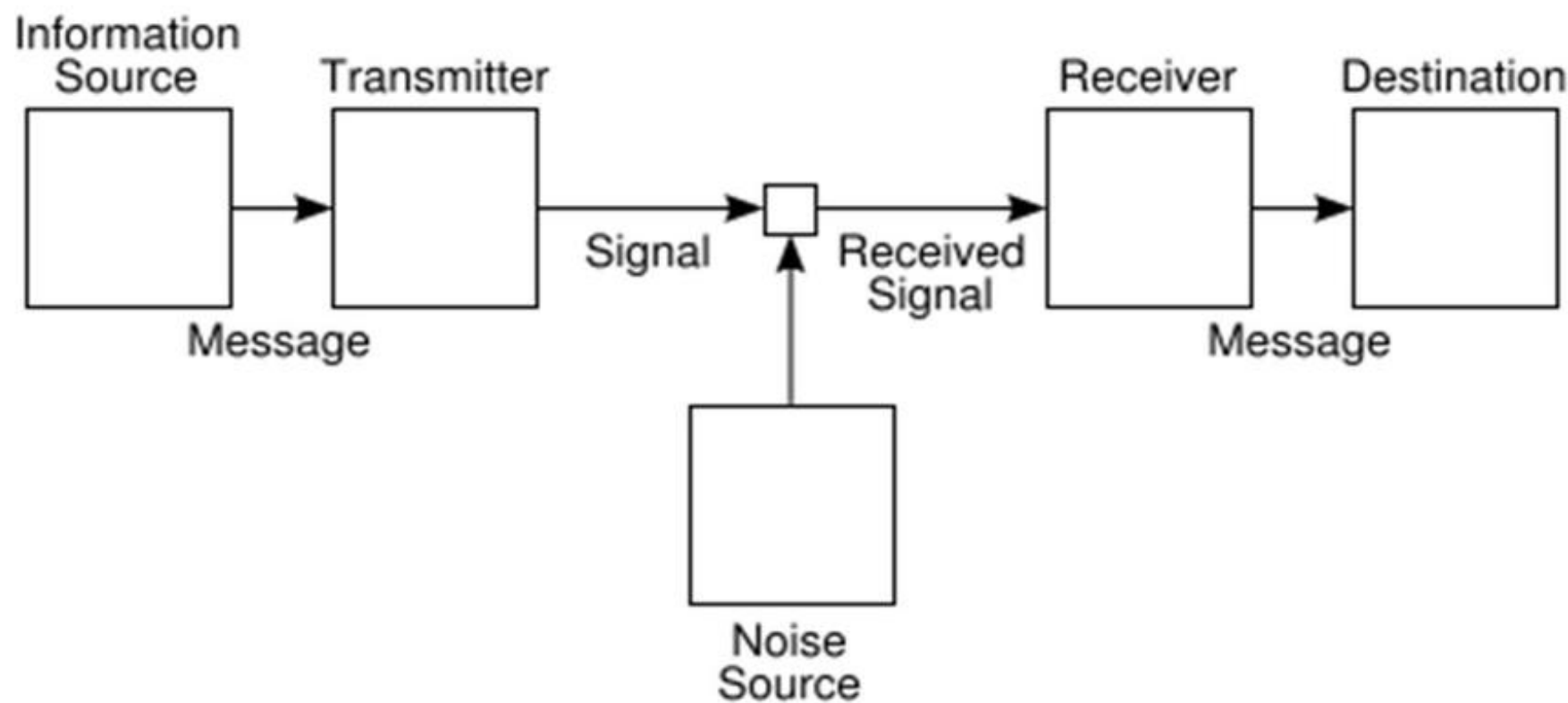
Population decoding



$$I_F = T \sum_i \frac{(m'_i(s))^2}{m_i(s)}$$



Information Theory



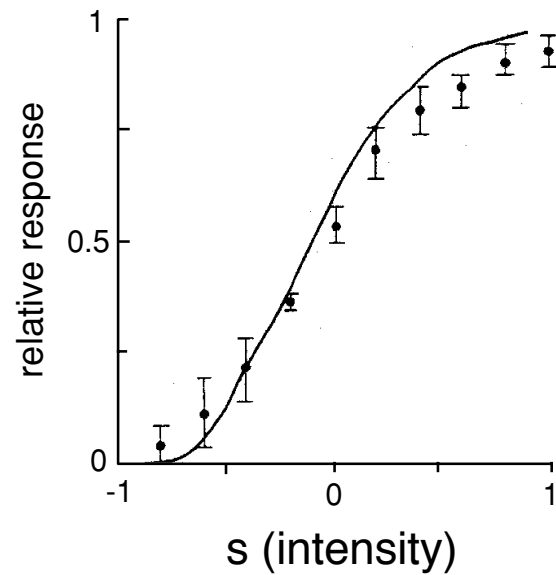
Shannon Information

The game of sixty three

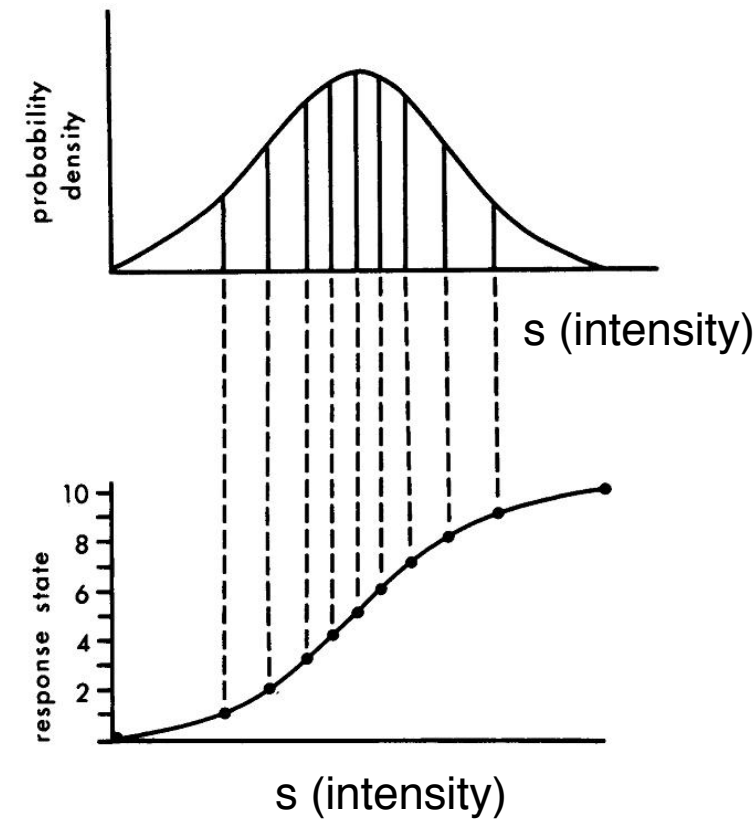
- $x \geq 32?$
- is $x \bmod 32 \geq 16?$
- is $x \bmod 16 \geq 8?$
- is $x \bmod 8 \geq 4?$
- is $x \bmod 4 \geq 2?$
- is $x \bmod 2 \geq 1?$

$$I = -\log_2 p$$

Maximizing entropy principle

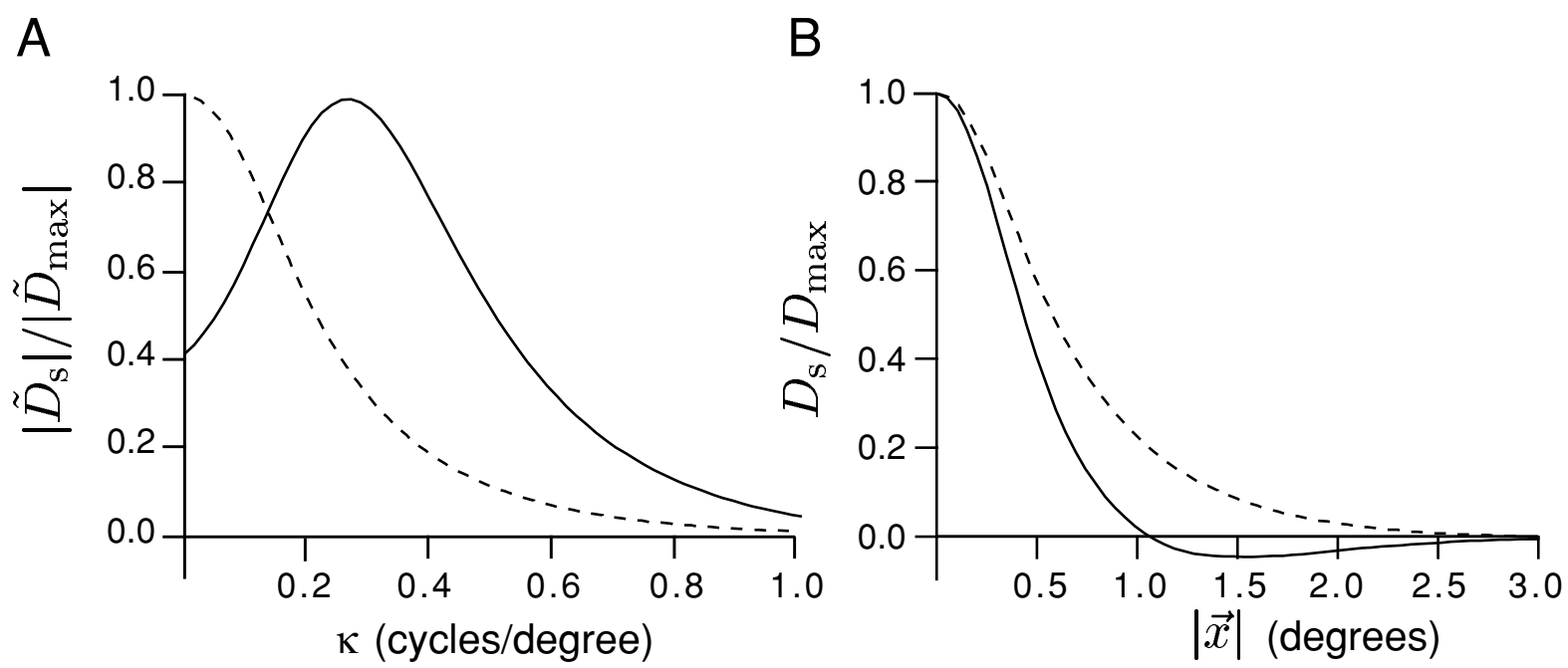


$$r = f(s)$$



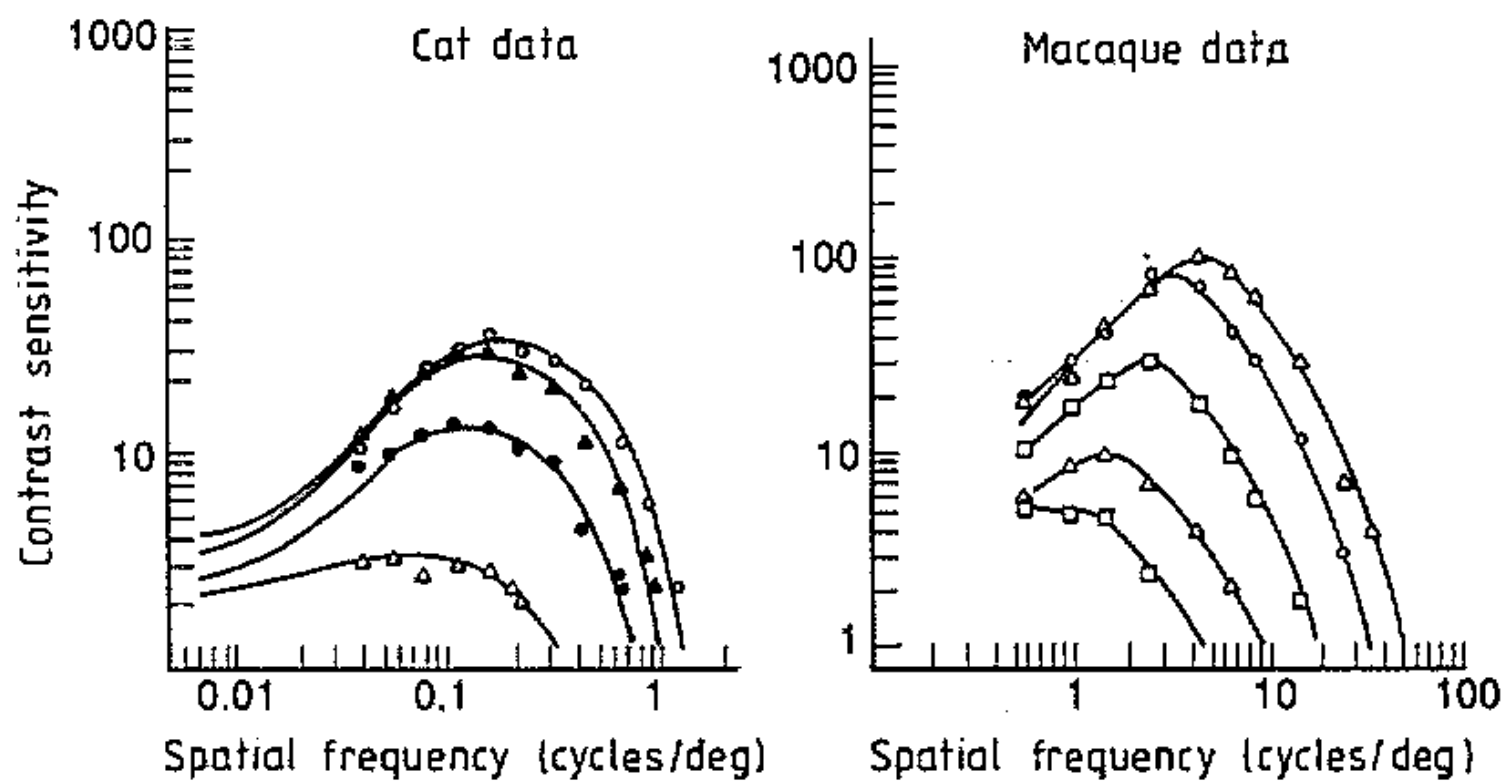
$$H = - \int_0^{r_{max}} dr p(r) \ln p(r) \quad \frac{df}{ds} = r_{max} p(s)$$

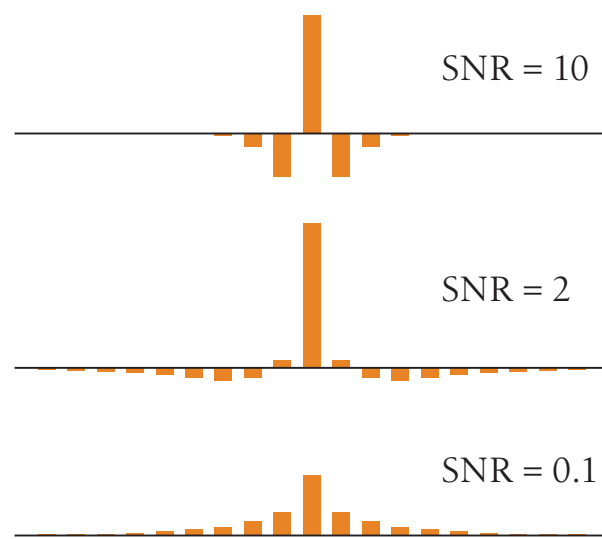
$$p(r) = \frac{1}{r_{max}}$$



232

J J Atick





(a)



(b)



FIGURE 6.33

Cross-sections through the optimal matrices W_{ij} in the problem of efficient coding with noise. The correlation function is assumed to be exponential, $C_{ij} \propto \exp(-|i - j|/\xi)$, with $\xi = 50$, much longer than the range of interactions shown here. At high signal-to-noise ratios (SNRs), the solution looks like a differentiator, which removes the second-order correlations in the signal, whereas at low SNR, the solution integrates to suppress noise. Redrawn from Atick and Redlich (1990).

